



Natalia Grabarczyk

## Food from the air: Selection and characterization of hydrogen oxidizing bacteria for sustainable anaerobic production of single-cell protein

MSc thesis | Department of Bioprocess Engineering | Wageningen University



**WAGENINGEN**  
UNIVERSITY & RESEARCH

---

# Food from the air: Selection and characterization of hydrogen oxidizing bacteria for sustainable anaerobic production of single-cell protein

---

by

Natalia Grabarczyk

A MSc thesis (BPE80336)

published at 3/8/2023

under the supervision of Carlos Serrano Fajardo and Giuseppe Olivieri

submitted to examiner Ruud Weusthuis

at the Department of Bioprocess Engineering, Wageningen University

in partial fulfilment of the requirements for the degree

Master of Science Biotechnology

---

# Abstract

---

Single-cell proteins (SCP) are an alternative source of protein that can be obtained from microbial biomass. The hydrogenotrophic cultivation has the potential to link the environmental sustainability with efficient production of SCP. The thesis aims to choose the most productive HOB cultivation method considering the energy efficiency of the respiration pathway and the best performing bacteria strain. The selection was meant to be done by comparing the yield of hydrogen on the biomass and the energy cost associated with the biomass production. To determine these values, the experimental setup was designed to autotrophically cultivate *Hydrogenophaga flava*, *Cupriavidus necator*, *Paracoccus denitrificans* and *Serpentinimonas barnesii* strains under aerobic and anaerobic conditions. Afterwards, bacterial cultures were analysed in terms of the consumption of the electron donor and acceptor as well as assimilation of the nitrogen and carbon source. The change in concentration of  $H_2$ ,  $O_2$ ,  $N_2$ ,  $NO_3^-$  and  $NH_4^+$  was measured. Furthermore, the total carbon and total nitrogen in the cell, biomass concentration and protein content were calculated, followed by the autotrophic *C. necator* growth rate determination. The experimental setup proved not to provide the reliable and consistent data, which were affected by the manual measurement errors, insufficient quality of the assay and a significant standard deviation between sample replicates. Therefore, the selection of the most energetically efficient HOB cultivation system could not be achieved. However, after identifying the shortcomings, improvement plan was suggested. This thesis serves as the basis for development of a suitable experiment design for further characterization of HOB.

*Keywords:* HOB, hydrogenotrophic cultivation, single-cell proteins, yield of hydrogen on biomass, energy efficiency, sustainability.

# Table of Contents

Abstract .....	ii
Nomenclature .....	3
Abbreviations .....	3
Symbols .....	3
1. Introduction .....	4
1.1. Food security and alternative proteins.....	4
1.2. SCP Production system .....	5
1.3. Aim of the thesis .....	8
1.4. Research Approach and Boundaries .....	8
2. Theoretical background .....	9
2.1. Denitrification and DNRA for anaerobic hydrogen respiration.....	9
2.2. HOB strains selected for the study .....	11
3. Materials and methods .....	13
3.1. Small scale cultivation of HOB.....	13
3.2. Sample analysis and data treatment .....	16
3.3. Batch reactor cultivation of <i>C. necator</i> $\Delta$ pha .....	20
3.4. Measurements .....	21
3.5. Data treatment of the batch experiment.....	21
4. Results.....	22
4.1. Biomass concentration and cell elemental composition .....	22
4.2. Biomass elemental composition.....	25
4.3. Gaseous substrates consumption.....	27
4.4. Nitrate yield.....	28
4.5. Ammonium yield .....	29
4.6. Protein content of the biomass .....	32
4.7. Biomass formation equation and energy cost .....	33
4.8. Batch reactor experiment .....	33
4.9. Growth rate of <i>C. necator</i> .....	33
5. Discussion and recommendations .....	35
5.1. Biomass concentration .....	35
5.2. Carbon content of the cell.....	36
5.3. Nitrogen content of the cell.....	37
5.4. Protein content .....	38
5.5. Gaseous substrates consumption.....	38
5.6. Ammonia yield .....	39
5.7. Nitrate yield.....	39
5.8. Growth rate in the batch cultivation .....	40
5.9. Biomass formation stoichiometry and energy cost .....	41

6. Conclusion ..... 42  
Acknowledgements..... 43  
References ..... 44  
Appendices ..... 48

# Nomenclature

---

## Abbreviations

BM	Biomass
CDW	Cell dry weight
CN	<i>C. necator</i> Δpha
DAC	Direct air capture
DNRA	Dissimilatory Nitrate Reduction to Ammonia
GC	Gas chromatography
HB	Haber Bosch
HF	<i>H. flava</i>
HOB	Hydrogen Oxidizing Bacteria
IC	Inorganic carbon
MFC	Mass flow controller
MS	Mass spectrometer
OD	Optical density
PD	<i>P. denitrificans</i>
PHA	Polyhydroxyalkanoate
SB	<i>S. barnesii</i>
SCP	Single cell protein
TC	Total carbon
TEM	Transmission electron microscope
TN	Total nitrogen
TOC	Total organic carbon
XRMA	X-ray microanalysis

## Symbols

$\mu$	Biomass growth rate
Y	Yield
$\Delta C$	Change in concentration
$\Delta G^0$	Standard Gibbs free energy
$\Delta H$	Enthalpy change
$\Delta H^0$	Standard enthalpy change

# 1. Introduction

---

## 1.1. Food security and alternative proteins

In recent years, there has been an increasing awareness of the negative impact of human activity on the environment. One of the main contributors to gradual exhaustion of natural resources and climate change is the food production system. Agriculture along with the arable land conversion are responsible for around 30 % of the greenhouse gas emissions. Furthermore, activities related to the food system decrease biodiversity and cause landscape pollution. Both crop and livestock farming require large input of water, fossil fuels for the energy purpose as well as availability of arable land [1]. The destructive influence of the food system proves to be not only a one-sided dependence. Climate change progression reduces the food production capacity through unpredictable weather events and rising temperature, whereas pollution deprives of the arable land and lowers quality of crops. With regard to a growing demand for food, it is estimated to increase by 70% by 2050 due to a continuously growing population. Therefore, neglecting transformation of the agricultural system poses a serious threat to the future food security. To mitigate the effects of Earth's exploitation, new solutions are needed. Methods of food production and its sources have to become significantly more environmentally sustainable [2].

Innovation in the global food system can be addressed by introducing an unconventional approach to dietary protein, for which the current demand reaches 202 million tonnes per year [3]. Animal derived protein such as cattle meat contributes to emission of a mean 50 kg CO<sub>2</sub> per 100 g protein, whereas the mean land use is equal 164 m<sup>2</sup>/year. By contrast, production of 100 g plant-based protein generates 2 kg of CO<sub>2</sub> by tofu and 0.8 kg CO<sub>2</sub> by pulses. The land use of plant protein requires 2.2 m<sup>2</sup>/year in case of tofu and 7.3 m<sup>2</sup>/year for pulses to obtain 100 g protein [4, 5]. In the light of these data, microbial protein which production requires less land and leaves a significantly lower carbon footprint, has received increasing attention in recent years.

Single cell proteins (SCP) refer to the edible proteins of bacteria, fungi and algae cells. They are suitable for dietary purpose due the rich amino acids profile. Bacteria amino acids profile has been compared to the fish protein, whereas SCP from yeast is similar to soya protein [6]. The examples of algae-derived SCP include spirulina, *Chlorella* and AlgaVia. Furthermore, myco-proteins have gained popularity thanks to the Quorn brand producing meat substitutes from *Fusarium venenatum* biomass as well as the spent brewer's yeast [7]. In terms of bacteria, proteins are almost exclusively processed for animal feed. For example, UniProtein and FeedKind produce supplements from biomass grown on methane. Even more interesting is the Solar Foods venture, which has been testing cultivation of bacteria for edible dietary protein, utilizing renewable energy and captured CO<sub>2</sub> [7, 8].

What makes the SCP a great alternative to plant and animal derived protein is the prospect of economically feasible and environmentally sustainable large-scale production. Referring to a land use issue, microbial cultivation may prove to be redeeming solution. SCP production system based on photovoltaic energy and CO<sub>2</sub> capture technology surpasses conventional cultivation methods. It can reach 13 times higher protein yield compared with soybean, not even to mention a few hundred times higher productivity than meat. Additionally, arable land is not required for microbial protein production, thus the facility will not occupy already scarce agricultural land [9]. By comparison, for every 100 g of protein produced, animal derived require 23 times more land than protein rich crops, whereas microbial SCP would use 15 times less land than plants (Figure 1) [4, 5, 9]. Moreover, when CO<sub>2</sub> is used as biomass feedstock, the whole process can potentially become carbon neutral. The anthropogenic CO<sub>2</sub> can be directly fed to microbes or converted to organic carbon sources after being captured from the air (DAC). Therefore, this would help to mitigate greenhouse gas emissions [10, 11]. Another advantage of SCP production via renewable energy and DAC is lower water usage, estimated to be tenfold less than soy requirement [12].

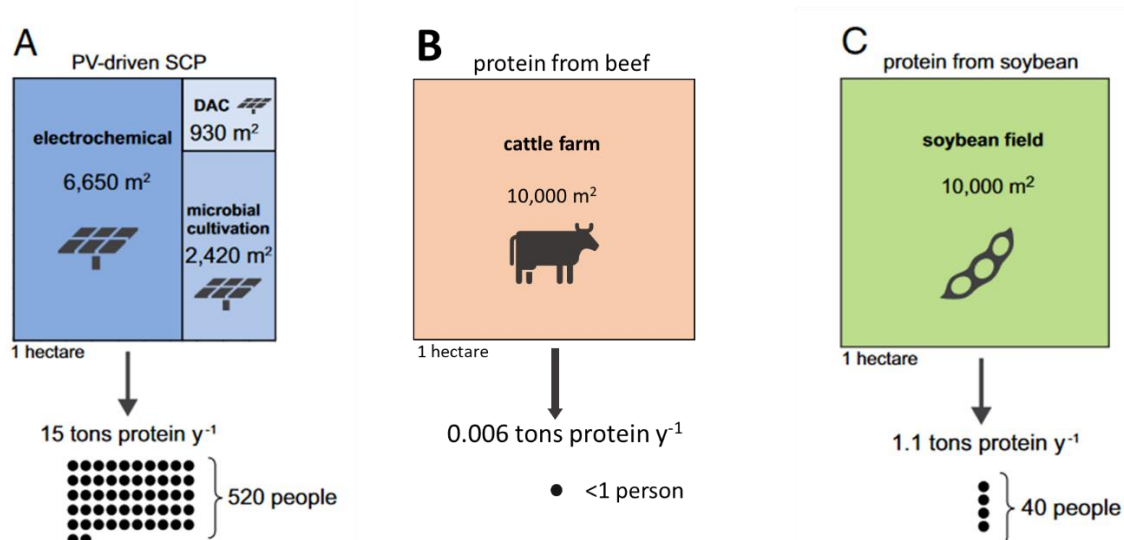


Figure 1 Comparison of land use and yearly protein yields to meet the daily human intake by different protein production approaches. One dot represents 10 people who daily consume 80 g of protein. Figure adapted from [4, 9].

Current food system requires transformation to tackle the future protein demand as well as an impact of climate change. A combination of green energy, DAC and bioreactors, could provide a promising alternative to crops and meat. Proteins from microbes would offer the resource-efficient, high yield, carbon neutral production strategy. However, the SCP production technology still requires significant development.

## 1.2. SCP Production system

Of the microorganisms capable of producing SCP, it would be essential to select those growing on  $CO_2$  and compounds obtained through renewable energy sources. Fortunately, the bacteria are known for their metabolic diversity. Hydrogen oxidizing bacteria (HOB) are capable of chemolithoautotrophic growth via hydrogen oxidation, serving as electron donor in respiratory chain. The released energy is further used to fix  $CO_2$  into biomass. Moreover, most HOB are facultative autotrophs, growing either on organic carbon or on  $H_2$  and  $CO_2$  mixture. In addition, the bacteria utilize oxygen, nitrate, sulphate, methane or even ferric ions as electron acceptors. This metabolic flexibility translates into their presence in unusual habitats such as hot hydrothermal vents [8, 13]. In the SCP cultivation setup, HOB biomass matures in the bioreactor to be harvested and purified for human consumption.

As it has been described, HOB SCP have significant advantages over traditional protein harvesting in terms of their potential for sustainable production. This is made possible mainly by using raw substrates generated from green energy or by directly extracting them from the air. The substrates obtained by these means include elemental hydrogen, oxygen, carbon dioxide and ammonia. Hydrogen along with oxygen can be produced via electrolysis process powered with solar photovoltaic energy or wind power. Furthermore, carbon source is provided by the DAC as  $CO_2$  [14]. Ammonia, the nitrogen source can be sustainably obtained via the Haber Bosch (HB) process, utilizing  $H_2$  and  $N_2$  captured from the air [15]. Additionally, vitamins and minerals are also supplied in small quantities [8, 16].

The production system designed in this way could successfully save more energy and resources, which can be even more facilitated by the conversion of respiration end products. Thereby, reducing costs and the amount of waste generated. The end product of electron acceptor reduction can undergo regeneration by oxidation with a suitable oxidant [17]. In case of aerobic cultivation, the by-product is water requiring no special treatment, whereas the means of regeneration of anaerobic respiration electron acceptors are discussed in 2.1.

In most HOB studies, cultivation is carried out under aerobic conditions [18-21]. The reason is high biomass yield from aerobic respiration process ensuring production efficiency. However, there are several disadvantages of aerobic respiration. First drawback is explosiveness of oxygen and hydrogen



mixtures, which affect safety of the process and hinders reactor design and the process scale-up [13]. Additionally, H<sub>2</sub> is poorly soluble in water which, combined with the safety ensuring low concentration, results in low gas-liquid mass transfer rates [22]. Currently, the cost of 1 kg H<sub>2</sub> generated via electrolysis and solar energy ranges between 2 and 6 euro [23]. Considering it accounts for more than 60 % of raw material costs, it is essential to use it efficiently [24].

In conclusion, the aerobic HOB cultivation is an efficient and proven method, however facing significant shortcomings with regard to the use of hydrogen, such as explosiveness and limited mass transfer. Therefore, there is a need of a process which would decrease the risk of explosion and overcome the mass transfer limitations. This could be achieved with an anaerobic cultivation approach.

In case of anaerobic respiration an electron acceptor can be present in the culture medium in ionic form, therefore the risk of explosion is avoided. Moreover, as higher concentration of H<sub>2</sub> is allowed, hydrogen mass transfer is facilitated as well. Of the compounds with the highest reduction potential that can compete with the energy released in the aerobic process, nitrate and ferric ions are the most suitable. Theoretically, the anaerobic hydrogen respiration could circumvent the issues of the aerobic system allowing for efficient use of electron donor. Nonetheless, the production of SCP from HOB utilizing the alternative electron acceptors such as nitrate remains an uncharted territory. The lack of empirical data does not allow to compare the yields of biomass on hydrogen and determine the most energetically efficient cultivation method [25].

Figures 2 and 3 briefly compare and summarize the aerobic and anaerobic cultivation processes. Both approaches utilize hydrogen obtained via the renewable energy and carbon source from the direct air capture. For anaerobic setups including nitrate as the electron acceptor and HOB capable of nitrogen assimilation from that source, ammonia produced by HB is not required.

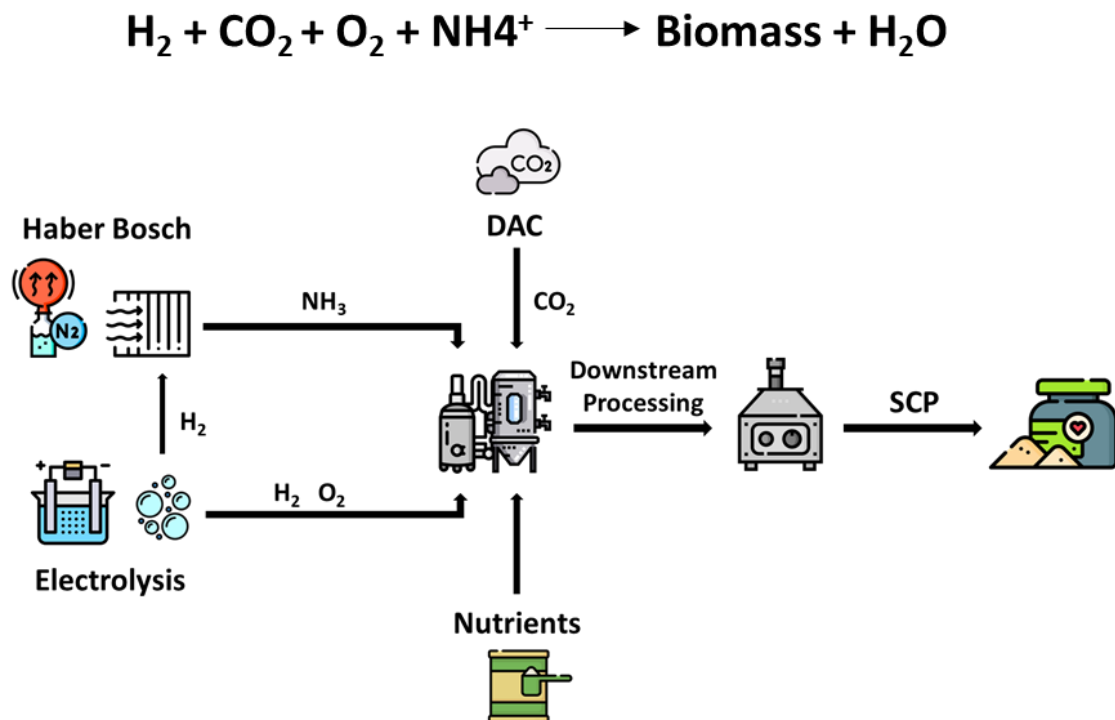


Figure 2 Simplified scheme of aerobic SCP production process from HOB. The bacteria undergo aerobic hydrogen respiration to gain energy necessary for fixation of CO<sub>2</sub>. Feedstock is obtained from the renewable energy sources and DAC.

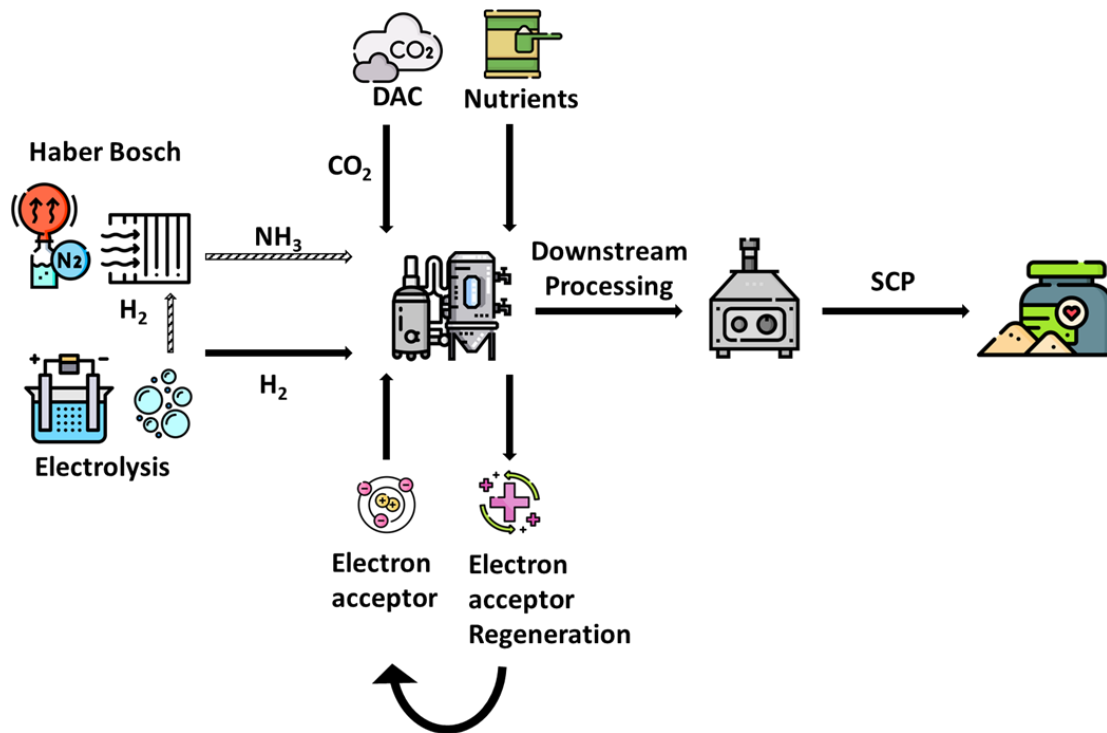


Figure 3 Simplified scheme of an anaerobic SCP production process from HOB. The bacteria undergo aerobic hydrogen respiration to gain energy necessary for fixation of  $\text{CO}_2$ . The electron acceptor is supplied to the bioreactor and after the reduction, its end-product is regenerated via oxidation. Ribbed arrows represent optional process for certain setups using HOB assimilation nitrogen from the electron acceptor.

### 1.3. Aim of the thesis

The main goal of the thesis is to select the most energetically efficient method of HOB cultivation including the respiration pathway and the best performing microorganism by comparing the yields of biomass on hydrogen of HOB grown autotrophically in aerobic and anaerobic conditions. The subject of cultivation regards HOB species gaining energy from hydrogen oxidation coupled with oxygen reduction, denitrification or DNRA. Obtaining these results will depend on the feasibility and reliability of the experimental design. This research aims to contribute to the development of an economically and environmentally sustainable SCP production system.

The main research questions to be addressed are as follows:

1. Is the experimental setup designed for this research suitable for HOB cultivation under aerobic and anaerobic conditions?
2. Do the chosen analytical procedures allow to obtain reliable and consistent data on the substrate consumption and biomass growth?
3. Which HOB species has the highest yield of biomass on hydrogen in aerobic and anaerobic conditions?
4. Which HOB cultivation method coupled with the electron acceptor recovery strategy is the most energetically efficient based on the empirical values of biomass formation enthalpy?

### 1.4. Research Approach and Boundaries

The experiments will focus on cultivation and characterization of 4 species of HOB including *C. necator*  $\Delta$ pha, *H. flava*, *P. denitrificans* and *S. barnesii*. These facultative aerobes are grown both in aerobic and anaerobic conditions, respiring hydrogen as the electron donor and utilizing CO<sub>2</sub> as the carbon source. Oxygen serves as the electron acceptor in case of aerobic cultivation, whereas nitrate is used as the alternative electron acceptor. Furthermore, *C. necator*  $\Delta$ pha is aerobically grown in the batch reactor to explore growth characteristics and compare the yields with smaller scale experimental setup. Afterwards, measurements of respiration process and biomass formation are done. Data is evaluated to determine the yields of biomass on hydrogen and electron acceptor, as well as cell composition and protein content. Furthermore, the reliability of the results will be assessed to determine whether this experimental setup is suitable for cultivation and qualitative analysis. If the design proves its suitability, integrated results will be used to determine the stoichiometric equation of biomass formation of each species. The equation enables to calculate the enthalpies which are the main criteria for selection of the most energetically efficient biomass production strategy.

One of the limitations the research has encountered is small scale of the experimental setup limiting biomass concentration and sample volumes. Considering the batch reactor, hydrogen concentration in the headspace is restricted by the safety measures. For this reason, H<sub>2</sub> is a limiting substrate, thus the most optimal conditions for growth could not be provided. Additionally, due to the time constraint the batch reactor run was performed once, what affects data credibility.

Other boundaries of the project include investigating only facultative aerobic HOB species. Strict anaerobes exhibiting good productivity on hydrogen are not researched due to the inability to obtain aerobic yields data, as well as demanding cultivation [26]. Moreover, it has to be mentioned that intermediate nitrogen compounds are not measured due to the time constraint and lack of suitable equipment. No online measurements except OD control for serum bottles experiment were taken either, as it would affect the gas composition in the headspace and volume of culture broth.

## 2. Theoretical background

---

This chapter takes a closer look on anaerobic hydrogen respiration with nitrate as an electron acceptor. Moreover, the challenges of anaerobic HOB cultivation are addressed along with a description of the microorganisms used in this study.

### 2.1. Denitrification and DNRA for anaerobic hydrogen respiration

One of the promising electron acceptors in HOB anaerobic respiration process is nitrate. The ion can be reduced and generate the proton motive force essential for ATP synthesis. Even though the  $\text{NO}_3^-$  reduction potential is lower than that of oxygen, the multi-step reduction reaction still allows the release of a significant amount of energy required for biomass growth. Reduction of nitrate can follow different pathways including denitrification, anammox and dissimilatory nitrate reduction to ammonium (DNRA). The end product of the first two paths is dinitrogen, whereas DNRA yields ammonium [27].

Hydrogenotrophic denitrification consists of four separate enzymatic reactions. At first, nitrate is reduced to nitrite by the Nar/Nap complex bound to the cell membrane. Afterwards, nitrite is converted to nitric oxide by the Nir complex family located in the periplasm. Nitric oxide undergoes reduction to nitrous oxide by the Nor complex family. Finally, dinitrogen is the product of nitrous oxide conversion facilitated by NosZ complex [28, 29]. The reactions in this process are shown in the following equations (1-4).



In DNRA, nitrate is reduced to ammonium. First step of nitrate reduction is catalysed in periplasmic membrane by the Nap, although the reduction can also be done by the Nar complex. Furthermore, nitrite is reduced to ammonium by NrfA periplasm complex [28, 29]. Therefore, full DNRA can be described by two redox reactions presented in the equations (5-6).



Both anaerobic pathways using nitrate as an electron acceptor have one major drawback. The stoichiometric equations of oxygen and nitrate redox reactions show the difference in the electrons transported (7-9). It is evident that reduction of 1 mole of  $\text{O}_2$  requires less protons than the nitrate reduction.



Looking at the redox tower (Figure 3) shows the lower reduction potential of nitrate redox reactions. The smaller the potential difference between the electron donor and acceptor, the less energy is available in the reaction. Translating the redox potential into the standard Gibbs energy of these reactions indicates that less energy is released per one proton regarding nitrate reduction (Table 1). For this reason, more hydrogen is expected to be needed for the anaerobic cultivation to generate the same amount of energy as in the aerobic process. More  $\text{H}_2$  means higher production costs.

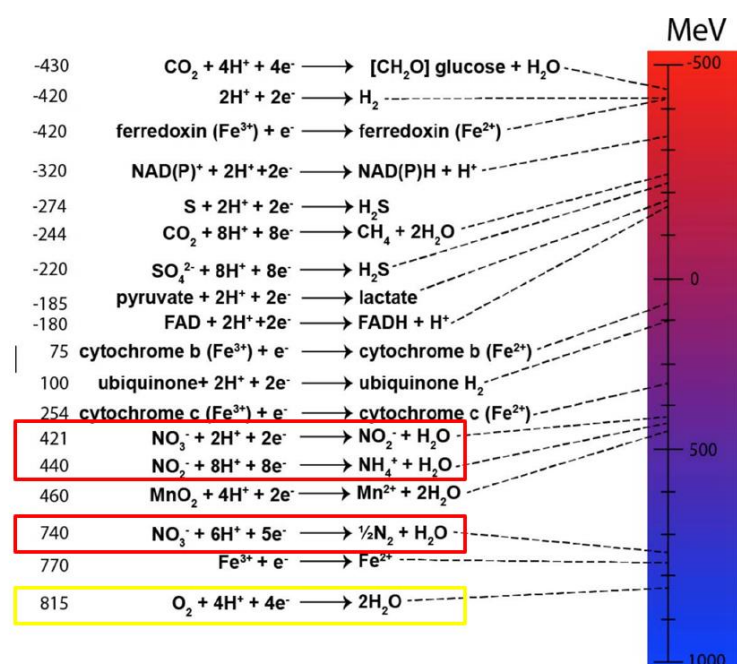


Figure 4 Redox tower presenting half reactions of different compounds. Nitrate and oxygen reduction are marked with yellow and red outlines. Megaelectron-volts (MeV) values are on the left side [30].

Table 1 The standard Gibbs free energy per one proton of chosen reduction reactions [16].

Reduction reaction	$\Delta G^0$ (kJ/H <sup>+</sup> )
$2NO_3^- + 10e^- + 12H^+ \rightarrow N_2 + 6H_2O$	-74.2
$NO_3^- + 8e^- + 10H^+ \rightarrow NH_4^+ + 3H_2O$	-68.2
$O_2 + 4e^- + 4H^+ \rightarrow 2H_2O$	-118.6

However, these energy values are only rough estimations as they are based only on standard values of chemical conversion. In the microbial cell the real available energy depends on the type of enzymes in the electron transport chain and their efficiency [31, 32]. Therefore, to gain a full insight into ATP yields of respiratory systems, empirical data is required.

To address the issue of energy efficiency of the anaerobic production while keeping in mind process sustainability, waste products need to be properly managed. Therefore, introduction of electron acceptor recovery could save the additional energy, and thus the energy balance will become more compensated in relation to aerobic respiration. Moreover, the issue of ammonia accumulation which becomes toxic in higher concentrations can be solved this way.

Regeneration of the electron can be done by oxidation of the respiration end-product, which releases energy if the form of heat. DNRA process yields ammonium which may be directly oxidized to nitrate. A chemical method called the Ostwald process, in which NH<sub>3</sub> is oxidized in two steps. Firstly, nitric oxide is formed through the reaction of NH<sub>3</sub> with oxygen and a catalyst. Afterwards, nitric oxide reacts with oxygen to synthesize nitrogen dioxide. In a reaction with water NO<sub>2</sub> is converted to nitric acid and nitric oxide [33]. The process steps are shown in the following reactions (10-12):



First oxidation step is an extremely exothermic reaction, operated at 600-800°C and under 4-10 bar pressure. The heat released from this process could be utilized to generate the energy required by other biomass production stages such as cooling of the bioreactor.

Besides the chemical regeneration, the by-products could possibly be used by diazotrophic cyanobacteria which convert gaseous nitrogen to ammonia [34]. Furthermore, the ammonia may be oxidized to nitric acid by the members of ammonia oxidizing bacteria including *Nitrospira* and *Nitrosomonas* [35]. Consequently, instead of heat, biomass is gained from which SCP or other valuable compounds can potentially be extracted.

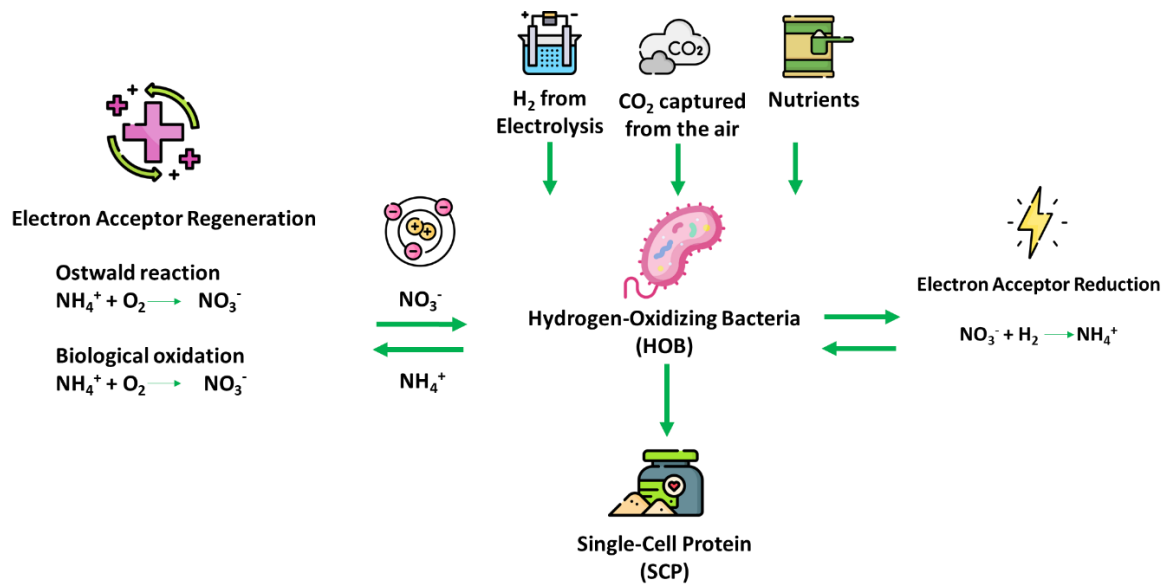


Figure 5 Scheme of the autotrophic anaerobic SCP production using  $\text{NO}_3^-$  as the electron acceptor. The system includes electron acceptor regeneration by biological or chemical oxidation.

## 2.2. HOB strains selected for the study

### 2.2.1. *C. necator*

*Cupriavidus necator* being one of the most studied HOB strains, belongs to a gram-negative *Betaproteobacteria* class. As a representative of autohydrogenotrophic microorganisms, it utilizes  $\text{H}_2$  and  $\text{CO}_2$  for growth. *C. necator* is a facultative aerobe, which switches its metabolism towards hydrogenotrophic denitrification in oxygen depleted conditions. Moreover,  $\text{CO}_2$  is assimilated in this bacterium by the Rubisco enzyme present in the Calvin cycle. Nitrogen can be sourced by *C. necator* from ammonia, urea and nitrogen gas. The species is known for production of polyhydroxyalkanoate (PHA), the biodegradable polymer. Regarding anaerobic respiration, *Cupriavidus* can utilize both  $\text{NO}_3^-$  and  $\text{NO}_2^-$  as terminal electron acceptor. Growth is possible on carbon sources including organic acids, fructose and carbon dioxide. The most suitable for protein production are strains with PHA knockouts, allowing to avoid the polymer accumulation in the cell [8, 36, 37].

### 2.2.2. *Hydrogenophaga flava*

*Hydrogenophaga flava* is a member of *Comamonadaceae* family and *Betaproteobacteria* class. It has been isolated from the niches such as wastewater or hot springs. It is described as a gram-negative bacterium with characteristic yellow pigmentation and recorded slow growth. *H. flava* is facultatively aerobic as well as exhibits chemolithoautotrophy. Both ammonium and nitrate can be used by the bacteria as nitrogen source for growth. Considering anaerobic respiration, denitrification activity was observed in this strain [38-40]. However, the presence of DNRA pathway is indicated by the UniProt search of closely related *H. pseudoflava*. Yet, the nitrite reductase (NAD(P)H) still must be determined in *H. flava* [41].

### 2.2.3. *Paracoccus denitrificans*

*Paracoccus denitrificans* represents the gram-negative bacteria of *Alphaproteobacteria* class. The bacteria are mostly isolated from soil or wastewater. *Paracoccus* is a non-fermentative facultative chemolithoautotroph which assimilates  $\text{CO}_2$  through the Calvin cycle. Moreover, it can utilize  $\text{NO}_3^-$ ,

$\text{NO}_2^-$  and  $\text{NH}_4^+$  as the nitrogen source. Anaerobic growth is facilitated by hydrogen or sulphur as an electron donor. The species is often researched due to its ability to switch from aerobic to anaerobic denitrification growth mode when oxygen becomes limiting and nitrate is present. In addition, nitrite could also be the initial reduction substrate. It is worth noting that it is a unique species due to its ability to replicate under hypergravity [42-45].

#### **2.2.4. *Serpentinimonas barnesii***

*Serpentinimonas* are gram-negative rods classified as members of *Comamonadaceae* family. The strain is closely related to *H. flava*. As the name suggests, *Serpentinimonas barnesii* inhabits serpentinization sites which are abundant in calcite, in other words calcium carbonate. Therefore, the strain is able to fix carbon from dissolved carbon dioxide via the Calvin cycle [46, 47]. The bacteria thrive in highly alkaline springs with pH between 10-11.5, what makes them the most alkalophilic prokaryote so far discovered. This resistance to high pH makes the bacteria a potentially useful organism for industry, as cultivation is exposed to a lower risk of contamination. In addition, the  $\text{NH}_3$  equilibrium is shifted towards the formation of gaseous ammonia, which is then more easily recovered. According to the genomic studies, *S. barnesii* utilizes  $\text{H}_2$  as an electron donor and prefers microaerobic conditions. Both oxygen and nitrate can serve as electron acceptors depending on cultivation conditions [48, 49]. It is not clearly established which pathway the nitrate is reduced in. Based on data on *Serpentinimonas* enzymes from UniProt database, a nitrite reductase (NAD(P)H) which reduces nitrite to ammonium is present as well as nitric oxide reductase. However, a nitrous oxide reductase has not been found, which indicates the possible DNRA pathway [41].

## 3. Materials and methods

### 3.1. Small scale cultivation of HOB

#### 3.1.1. Purpose

The aim of this experiment is to cultivate 4 chosen HOB strains in aerobic and anaerobic conditions to characterize and compare the growth and substrate consumption. Obtained data is used to determine biomass yield on electron donor and electron acceptors as well as further establishing of the enthalpy of biomass formation.

#### 3.1.2. Design

Bacteria strains were cultivated in 120 ml closed serum bottles with butyl rubber septum to avoid gas leakage and contamination. The first experimental run included *H. flava*, *P. denitrificans* and *S. barnesii*. The inoculated bottles were placed in the Algem HT24 photobioreactor, performing continuous OD measurements. In the 2<sup>nd</sup> run *C. necator*  $\Delta$ pha was grown in the ISF1-X Kuhner incubator shaker. Instead of a continuous OD check, the control samples were prepared, thus the culture broth samples were taken every day and their OD was checked. Furthermore, each strain was investigated under aerobic and anaerobic conditions, growing on an adjusted medium. The experimental bottles were prepared in triplicates or quadruplicates with an additional control sample containing only medium. The conditions applied for cultivation are presented in the Table 2.

Table 2 Cultivation conditions of serum bottle experiment on HOB.

Cultivation condition	<i>C. necator</i>	<i>H. flava</i>	<i>P. denitrificans</i>	<i>S. barnesii</i>
Temperature (°C)	30	30	30	30
pH	6.8-7	6.8-7	6.8-7	11
Shaking speed (rpm)	250	250	250	250
Culture broth volume (ml)	17	17	17	17
Medium	J minimal medium (JMM) [50]	Mineral medium for chemolithotrophic growth DSMZ 81	Mineral medium for chemolithotrophic growth DSMZ 81	Serpentinomonas minimal medium DSMZ 1634
Initial pressure (kPa)	101.325	101.325	101.325	101.325
Time of incubation (days)	7-14	5-8	5-8	5-8

The number of samples and setup of 1<sup>st</sup> and 2<sup>nd</sup> experimental run were adapted to the incubator's capacities. Table 3 Table 4 present the distribution of samples in the runs.

Table 3 Algem HT24 experimental setup (HF – *H. flava*; PD – *P. denitrificans*; SB – *S. barnesii*). Control samples contain only medium. Aerobic samples are labelled with O letter, whereas anaerobic samples have N letter.

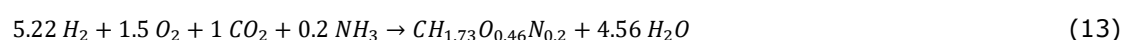
HF control O	HF control N	PD control O	PD control N	SB control O	SB control N
HF O1	HF N1	PD O1	PD N1	SB O1	SB N1
HF O2	HF N2	PD O2	PD N2	SB O2	SB N1
HF O3	HF N3	PD O3	PD N3	SB O3	SB N1



Table 4 Incubator setup for *C. necator*  $\Delta$ pha run (CN - *C. necator*  $\Delta$ pha). Control samples are the medium samples without inoculum. Aerobic samples are marked with a letter O, N represents samples with  $KNO_3$  only medium and NN indicate samples with  $NH_4$  and  $NO_3$  in medium.

CN OD control	CN control O	CN O1	CN O2	CN O3	CN O3
CN OD control	CN control N	CN N1	CN N2	CN N3	CN N4
CN OD control	CN control NN	CN NN1	CN NN2	CN NN3	CN NN4

Concentrations and volumes of gases in the bottle headspace were calculated from the stoichiometric equation serving as an estimation of the amount sufficient to reach the biomass concentration of 0.25 g/L. The approximate values of biomass concentration and corresponding OD values are based on data from autotrophic and heterotrophic *C. necator* growth studies [24, 51]. The stoichiometry of biomass formation is based on the equation 13 [52]:



The gaseous reagents and aqueous electron acceptor concentrations can be found in the Appendix 1. Chosen  $CO_2$  concentration is used in common cultivation practice for chemoautotrophic microorganisms [13, 53]. Furthermore, to facilitate the respiration process, a higher concentration of hydrogen was chosen at the expense of oxygen. However, gas mixtures of  $H_2$  and  $O_2$  become flammable and even explosive in range of certain concentrations. Therefore, to comply with safety regulations, the oxygen concentration did not exceed a threshold of 6 % in the aerobic cultivation samples [21, 54]. Table 5 shows the composition of gas mixture in the experimental bottles.

Table 5 Gas concentrations in the experimental bottle's headspace.

Gas composition (%)	Aerobic cultivation	Anaerobic cultivation
$H_2$	21	21
$O_2$	6	0
$CO_2$	10	10
$N_2$	64	69

A test run using *C. necator* was also performed. However, the suitable conditions were not provided followed by errors in post-harvest measurements, thus the results of this run will not be discussed. Nevertheless, the mistakes made during that cultivation made it possible to improve the design of further experiments. Therefore, detailed information and supplementary data about all experimental runs can be found in the Appendix 1.

### 3.1.3. Microorganism cultivation

This study used 4 species of facultatively aerobic HOB. *Cupriavidus necator* H16\_ $\Delta$ phaC was acquired from the Microbiology Laboratory at the Wageningen University. The strain does not produce PHA as a result of phaC1 and phaC2 genes knockout [55]. The colony used for the starter culture came from the previously prepared cryostock. Bacteria ordered from DSMZ include *Serpentinimonas barnesii* H1 (DSM103920), *Paracoccus denitrificans* (DSM413) and *Hydrogenophaga flava* (DSM619) delivered as lyophilizates.

The colony of *C. necator* from cryostock vial was recovered in Erlenmeyer containing 20 ml of JMM3 medium with fructose addition (20 g/L). After 2 days, 10 ml of the starter culture was transferred to the flask with 100 ml of medium with fructose. Freeze dried cultures were removed from the glass ampoules and the suitable medium was added to the pellet to resuspend it. Cell suspension of *H. flava* and *P. denitrificans* were transferred to the Erlenmeyer flasks containing 100 ml of fresh medium supplemented with glucose (20 g/L). Following the recommendations given in the medium's recipe, *S. barnesii* culture was injected to the closed serum bottle, previously flushed with 30% air, 50%  $H_2$  and 20 %  $N_2$ . The inoculated flasks were incubated in a Kuhner shaker at 30 °C 60, rotating at 250 rpm for 7 days. Thereafter, 1 ml of culture broth from every strain was collected and mixed with 1 ml of sterilized 50 % glycerine stock in an Eppendorf tube to be cryopreserved at -80 °C.

The media for microbial cultivation were chosen according to the DSMZ database recommendations. The medium composition for *C. necator*  $\Delta$ pha cultivation has been adapted from Liu 2012 study [50]. Media were adjusted for anaerobic cultivation by substituting the nitrogen source with  $\text{KNO}_3$ . Additionally, for *C. necator* cultivation 3 conditions were introduced, one aerobic and two anaerobic. In the anaerobic setup, the one medium contained  $\text{KNO}_3$  as a sole nitrogen source, whereas the other included both  $\text{NH}_4\text{Cl}$  and  $\text{KNO}_3$ . The purpose of the second setup was to compare on which nitrogen source *C. necator* growth is better facilitated.

Table 6 summarizes the substrates used in 3 cultivation conditions.

Table 6 Description of substrates for carbon fixation and respiration regarding each cultivation condition.

Cultivation condition	Aerobic	Anaerobic 1	Anaerobic 2
Strains	<i>H. flava</i> , <i>P. denitrificans</i> , <i>S. barnesii</i> , <i>C. necator</i> $\Delta$ pha	<i>H. flava</i> , <i>P. denitrificans</i> , <i>S. barnesii</i> , <i>C. necator</i> $\Delta$ pha	<i>C. necator</i> $\Delta$ pha
Carbon source	$\text{CO}_2$	$\text{CO}_2$	$\text{CO}_2$
Nitrogen source	$\text{NH}_4$	$\text{NO}_3$	$\text{NH}_4 + \text{NO}_3$
Electron donor	$\text{H}_2$	$\text{H}_2$	$\text{H}_2$
Electron acceptor	$\text{O}_2$	$\text{NO}_3$	$\text{NO}_3$
Reducing agent	no	yes	Yes
Resazurin	no	yes	yes

To ensure anoxic conditions, resazurin solution was added to the medium purposed for anaerobic cultivation. After addition of the anoxic indicator, medium initially turned violet (Figure 6). The colour of the medium changed back to transparent after the gas exchange and providing a reducing agent L-cysteine HCl during inoculation.



Figure 6 Medium with resazurin solution in oxygen (on the left) and anoxic conditions (on the right).

Before the start of an experiment, starter cultures had been centrifuged with the supernatant discarded. Pellets were then resuspended in a fresh medium without any carbon source. For the experiment, the bottles with medium were closed and made anoxic by flushing with nitrogen using KNF SC920 vacuum pump connected to the flushing station. Afterwards, the gas exchange was performed using mass flow controllers supplying gases through the tubes connected to the bottles via needles. The outlet tube led to MS which displayed the current gas concentration in the mixture. Then, 250  $\mu\text{l}$  gas samples from each bottle were taken for Gas Chromatography (GC) assay. Pressure in the vials was checked with manometer. Finally, the bottles were autoclaved and after they cooled down, inoculum with filtered vitamins, reducing agent and temperature sensitive compounds was injected to the bottles. Once the contents have been mixed, an initial sample of culture broth was taken. Depending on the experiment run, flasks were placed either in Algem HT24 bioreactor or in an orbital shaker incubator. The experiments lasted 5 - 8 days for 1<sup>st</sup> run and 7-14 days for 2<sup>nd</sup> run and they were stopped after no growth was observed.

### 3.1.4. Sampling

Sampling was performed in a downflow cabinet. Initial 4 ml broth sample was used for TC/TN, NO<sub>3</sub>, NH<sub>4</sub> assays as well as OD measurements. Before harvesting the culture broth, pressure in the bottles was recorded and gas samples were taken using GC. First, the liquid broth was collected from the serum bottle and distributed to tubes for the analyses. The tubes were put in the fridge to hinder bacterial metabolism. Harvested 17 ml of broth was used for the same assays as the initial sample. Moreover, CDW measurement along with determination of protein content was carried out.

## 3.2. Sample analysis and data treatment

### 3.2.1. Gaseous substrates consumption

Composition of gas reagents was determined with the use of Shimadzu GC 2014 at the Microbiology Department at the Wageningen University. The chromatography column analysed H<sub>2</sub>, O<sub>2</sub> and N<sub>2</sub> in the gas samples. Every sample contained 250 µl of gas from the experimental bottle. Standards were prepared by filling closed serum bottles with 100 % concentration of three analysed gases at atmospheric pressure. A syringe with a valve was used to collect samples. Between each measurement, the syringe was flushed with air to discard residual gas.

Peaks of the gases detected with the GC column were manually integrated in the ThermoFisher Chromeleon software with established gas processing method including retention time of standards (Appendix 2). Data showed the percentage of sampled gas volume relative to the corresponding standard of O<sub>2</sub>, N<sub>2</sub> or H<sub>2</sub> occupying the total volume of the bottle headspace. Assuming ideal gas behaviour, these values were converted to moles considering the pressure inside the experimental bottle. Average of sample replicates from the final measurement was taken. The substrate consumption is equal to the difference in the number of moles of gas in the bottle before and after the experiment. Moreover, the consumption efficiency was calculated by dividing the consumed reagent over the initial amount of a gas compound in the bottle.

### 3.2.2. Biomass concentration

Concentration of biomass was determined using the filter drying method. Filters were pre-treated by flushing with water to remove binder and left to dry in the oven. Culture broth samples were filtered through Ø 45 mm Whatman glass microfibre filter GF/F with 0.7 µm pore size and left in the oven for 24 hours at 100 °C. Afterwards, the filter papers were transferred to a desiccator for 2 hours and weighed on an analytical balance. Moreover, the OD of both initial and harvest cultures was measured. Starter cultures concentrations at different dilutions were also analysed with the filter drying and OD measurements.

Biomass (BM) concentration was determined with the use of OD and CDW data from filter-drying. Initial biomass concentration was estimated using the standard curves of OD/CDW prepared from the starter cultures of examined HOB. The biomass concentration was calculated according to the Equation 13. Additionally, OD measured at the end of the experiment was calculated to concentration to compare with the filter drying results. The biomass growth ( $\Delta$ CDW) during the experiment is described by equation 14.

$$\Delta CDW = Final\ biomass\ conc. - Initial\ biomass\ conc. \quad (14)$$

### 3.2.3. Protein content

Protein content of bacteria species was examined by means of Lowry assay. This analytical method combines Biuret and Folin-Ciocalteu reactions. The proteins' peptide bonds react with copper under alkaline conditions creating copper ionic complex. The ion catalyses the reaction of Folin reagent which reduction leads to formation of blue colour. The colour intensity depends on tyrosine, cysteine, histidine, asparagine and tryptophan content of the biomass [56]. Protein standard curve was prepared with BSA diluted in demiwat in the concentration range between 0 and 1000 µg/ml. This range has been chosen because of predicted low protein concentration in the samples as well as the loss of BSA linearity above 1 mg/ml [57].

Determination of total protein content was performed using harvested culture broth samples. The broth was centrifuged along with the supernatant discarded followed by resuspension in

demiwater. This step was done exclude interfering compounds. Afterwards, the sample was transferred to a lysing matrix D and run in a beat beating homogenizer. Finally, the samples were pipetted in triplicates to a 96-well microplate, mixed with the reagents from Bio-Rad Dc protein assay kit and left to incubate for 30 min. Absorbance was measured at 750 nm using Tecan M200 Plate Reader.

The average of the obtained OD replicates was taken and multiplied by a correction factor, which accounted for the concentration of the sample after the supernatant washout step. The protein concentration was calculated using the BSA standard curve. The outcome results were used to obtain the protein content in the biomass (15).

$$\text{Protein content} = \text{protein concentration (g/L)} / \text{biomass concentration (g/L)} \quad (15)$$

### 3.2.4. Nitrate yield on the biomass

Nitrate concentration was evaluated via the colorimetric assay. The reaction involves reduction of  $\text{NO}_3^-$  by copperized cadmium coil to  $\text{NO}_2^-$ . Furthermore,  $\text{NO}_2^-$  reacts with sulphanilamide creating a complex which couples with NED (N-naphthyl-ethylenediamine dihydrochloride) to form pink azo dye. The absorbance of this compound is measured at 520 nm [58].

Collected supernatant of the culture broth was tested via the AQ2 Seal Nutrient Analyser. The samples were manually diluted 3x with demiwater and the automatic dilution of 60x was applied to fit in the method detection range. The assay gives results expressed in mg  $\text{NO}_3^-$ /L.

The nutrient analyser provides already calculated concentrations of nitrogen nitrate in the samples. The calibration curve in the 0.05-15 mg N/L concentration range, had a correlation coefficient of 0.9997 (Appendix 3). To ensure the accuracy of the measurements, control tests were also carried out at known nitrate concentrations. Dilution factor was automatically included in the measurements. The results were converted to nitrate concentration. Furthermore, the difference in  $\text{NO}_3^-$  concentration between the initial and the end point sample was calculated. Finally, the yield of  $\text{NO}_3^-$  on biomass will be calculated according to the Equation 16.

$$Y_{\text{NO}_3\text{X}} = \frac{\Delta C_{\text{NO}_3}}{\Delta C_{\text{X}}} \left( \text{g NO}_3 / \text{g BM} \right) \quad (16)$$

$Y_{\text{NO}_3\text{X}}$  – Yield of nitrate on the biomass ( $\text{g NO}_3 / \text{g BM}$ )

$\Delta C_{\text{NO}_3}$  – difference between initial and final  $\text{NO}_3^-$  concentration ( $\text{g/L}$ )

$\Delta C_{\text{X}}$  – difference between initial and final biomass concentration ( $\text{g/L}$ )

### 3.2.5. Ammonia yield on the biomass

Ammonium concentration in the medium was found with the Spectroquant Ammonium Test determining ammonium nitrogen in the range of 2-150 mg/L. Ammonium in highly alkaline solution reacts with hypochlorite ions to form monochloramine. The amine reaction with phenol results in a dark green compound, which is spectrophotometrically measured at 690 nm [59].

Supernatant samples were appropriately diluted before the assay depending on the expected  $\text{NH}_4^+$  concentration to fit the standard curve prepared with  $\text{NH}_4\text{Cl}$  solutions range between 0 and 100 mg  $\text{NH}_4^-$  N/L. Firstly, the samples were mixed with reagent 1 and then reagent 2. Incubation time was 15 min. The solution was additionally diluted and transferred to the cuvettes to be measured in the spectrophotometer.

The colorimetric assay provided OD data which from which the average was converted into the concentration of ammonia nitrogen (mg/L) using the calibration curve with a correlation coefficient of 0.982. The results were further converted to ammonia concentration (mg/L). Consumption of ammonia in the medium was estimated by calculating the difference between the initial and final  $\text{NH}_4^+$  concentrations. Moreover, the yield of  $\text{NH}_4^+$  on biomass was determined (17).

$$Y_{NH_4X} = \frac{\Delta C_{NH_4}}{\Delta C_X} (g \text{ NH}_4 / g \text{ BM}) \quad (17)$$

$Y_{NH_4X}$  – Yield of ammonium on the biomass ( $g \text{ NH}_4^+ / g \text{ BM}$ )

$\Delta C_{NH_4}$  – difference between initial and final  $\text{NH}_4^+$  concentration ( $g/L$ )

$\Delta C_X$  – difference between initial and final biomass concentration ( $g/L$ )

### 3.2.6. Biomass elemental composition and $\text{CO}_2$ consumption – TC/TN analysis

Total organic carbon (TOC) and total nitrogen (TN) were determined with the Shimadzu TOC-L/TN-L analyser. It measures all organically bound carbon as well as dissolved nitrogen species and biomass bound nitrogen. The detection range is up to 1 g/L for carbon and 0.1 g/L nitrogen, thus the samples must be adequately diluted. In order to purge the inorganic carbon, samples were acidified with 0.0267M HCl solution and degassed in a sonification water bath for 20 min at 37 kHz frequency and power of 100 W. TC analysis was carried out for culture broth and supernatant, whereas TN was measured only from the supernatant samples.

The change of biomass-associated carbon and nitrogen was calculated.  $\text{CO}_2$  consumption relates to the consumption of carbon given by the difference between initial and final carbon concentration in the culture broth, normalizing for the initial C content in the cultivation media. Moreover, the results were corrected with the error factor of a control standard sample. Total nitrogen data contains both the ammonia and nitrate present in the culture supernatant. The average elemental biomass composition was determined by calculating the content of carbon and nitrogen in the initial and final samples. The biomass elemental composition is represented by the formula  $C_xH_yO_zN_w$ , whose carbon and nitrogen content can be calculated using the equations (18,19).

$$C \text{ content } \left( \text{mol C} / \text{mol BM} \right) = \frac{c_C \left( \frac{g}{L} \right)}{c_X \left( \frac{g}{L} \right)} \times 24.8 \frac{\frac{g}{\text{mol}}}{12.01} \left( \frac{g}{\text{mol}} \right) \quad (18)$$

$$N \text{ content } \left( \text{mol C} / \text{mol BM} \right) = \frac{c_N \left( \frac{g}{L} \right)}{c_X \left( \frac{g}{L} \right)} \times 24.8 \frac{\frac{g}{\text{mol}}}{14.0067} \left( \frac{g}{\text{mol}} \right) \quad (19)$$

$C_X$  – total organic carbon concentration ( $\frac{g}{L}$ )

$C_N$  – total nitrogen concentration ( $\frac{g}{L}$ )

$C_X$  – biomass concentration ( $\frac{g}{L}$ )

### 3.2.7. Observed yield of biomass on hydrogen

From the established stoichiometry of biomass formation reaction, the yield on hydrogen could be calculated. The yield is obtained from the following equation (20):

$$Y_{XH} = \frac{\Delta C_X}{\Delta H_2} \left( \text{mol BM} / \text{mol H}_2 \right) \quad (20)$$

$Y_{XH}$  – Yield of biomass on hydrogen ( $\text{mol BM} / \text{mol H}_2$ )

$\Delta C_X$  – difference between initial and final biomass concentration ( $\text{mol}/L$ )

$\Delta H_2$  – difference between initial and final hydrogen concentration ( $\text{mol}/L$ )

The amount of hydrogen required to produce 1 C-mol biomass is integrated in the energy cost of hydrogen generation via electrolysis.

### 3.2.8. Biomass formation equation stoichiometry

The stoichiometric coefficients of every reagent in the biomass formation equation could be established by normalizing all the data to C-moles of biomass produced. The results of the previous analyses were combined into a single equation and balanced with water and protons. It is assumed that there are no other by-products except water, ammonia and nitrogen in case of the anaerobic growth. Furthermore, the enthalpy of the biomass formation reaction was calculated by applying the Hess Law (21) as well as using the values of standard enthalpy of formation for the reagents. Due to the fact that the standard enthalpies of formation do not correspond to exact physiological conditions, the calculated reaction enthalpy is a simplification of the real enthalpy value affected by change in pH and ionic strength.

$$\Delta H = \sum n_i \Delta H_f^0(\text{products}) - \sum n_i \Delta H_f^0(\text{reactants}) \quad (21)$$

$$\Delta H - \text{standard enthalpy of the reaction} \left( \frac{\text{kJ}}{\text{C}} - \text{mol} \right)$$

$n_i$  – stoichiometric coefficient

$$\Delta H_f^0 - \text{standard enthalpy of formation} \left( \frac{\text{kJ}}{\text{mol}} \right)$$

### 3.2.9. Energy cost of the process

The energy cost estimation focuses on establishing the energy released during HOB cultivation, the energy required for hydrogen electrolysis and the additional energy gained from the electron acceptor recovery. The energy input of the other production steps has already been established in the literature [17]. Therefore, the enthalpy of biomass formation reaction, the yield of biomass on hydrogen as well as the yield of ammonia on biomass is used to determine the energy with the following equations (22 - 27). The electrolysis efficiency is assumed to reach 70 %, whereas the Ostwald and HB processes can achieve 97 % efficiency [60, 61].

$$\text{Energy for cooling} = -\Delta H \text{ biomass formation} \left( \frac{\text{kJ}}{\text{C}} - \text{mol} \right) \quad (22)$$

$$\text{Energy for water electrolysis} = \text{efficiency} \times \frac{\Delta G \text{ electrolysis}}{2} \left( \frac{\text{kJ}}{\text{mol H}_2} \right) \quad (23)$$

$$\text{Energy for H}_2 \text{ production} = Y_{\text{H}_2\text{x}} \left( \frac{\text{mol H}_2}{\text{C}} - \text{mol} \right) \times \text{water electrolysis} \left( \frac{\text{kJ}}{\text{mol H}_2} \right) \quad (24)$$

$$\text{Energy from the electron acceptor recovery} = \text{Ostwald process} \left( \frac{\text{kJ}}{\text{mol}} \right) - \text{HB process} \left( \frac{\text{kJ}}{\text{mol}} \right) \quad (25)$$

$$\text{Ostwald process energy} = \text{NH}_4^+ \text{ production} \left( \frac{\text{mol}}{\text{C}} - \text{mol} \right) \times \Delta H \text{ Ostwald process} \left( \frac{\text{kJ}}{\text{mol}} \right) \quad (26)$$

$$\text{HB process} = \text{NH}_4^+ \text{ consumption} \left( \frac{\text{kJ}}{\text{mol}} \right) \times \Delta H \text{ HB process} \left( \frac{\text{kJ}}{\text{mol}} \right) \quad (27)$$

$$\Delta H - \text{standart enthalphy} \left( \frac{\text{kJ}}{\text{C}} - \text{mol} \right)$$

$$\Delta G^0 - \text{standard Gibbs free energy} \left( \frac{\text{kJ}}{\text{mol}} \right)$$

$$Y_{\text{H}_2\text{x}} - \text{Yield of hydrogen on the biomass} \left( \frac{\text{mol H}_2}{\text{C}} - \text{mol} \right)$$

The detailed protocols for all the assays are available in eLabJournal. Data sheets containing the assay results and calculations can be found in the Appendix 1.

### 3.3. Batch reactor cultivation of *C. necator* Δpha

#### 3.3.1. Purpose

The reactor experiment aims to determine the growth rate and biomass protein content of *C. necator* Δpha autotrophic culture grown in aerobic conditions. Moreover, the yield of biomass on hydrogen is meant to be found. The experiment would allow to compare the growth characteristics and respiration efficiency of *C. necator* in upscaled cultivation setup with the serum bottle experiment.

#### 3.3.2. Design

*C. necator* Δpha has been grown autotrophically on hydrogen in presence of oxygen. The experiment run only once due to time constraint and lasted 5 days. The cultivation conditions are presented in the Table 7. The reactor run was performed in a full batch operation mode, both for the liquid and gas phase. To achieve the sufficient gas volume for growth, a 10 L Linde Plastigas bag was used. The polyethylene-aluminium coated bag does not permeate hydrogen. The bag was connected with the reactor headspace inlet tube. Gas exchange supplied with mass flow controllers was performed to set required gas composition and volume. Moreover, a Unisense hydrogen microsensor was monitoring H<sub>2</sub> concentration during the gas exchange.

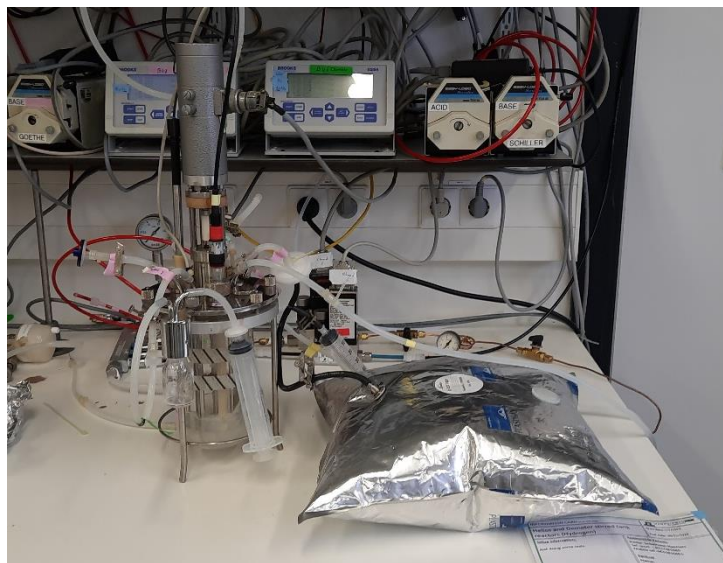


Figure 7 Batch reactor setup.

The experiment was carried out in a 1.2 litre stirred tank reactor, which working volume was 400 ml. The total headspace for gases including the reactor and the bag reached 10.85 litre. The reactor was controlled via ADI 1030 BioController. Furthermore, temperature, pH and hydrogen concentration in the headspace were monitored in-line via sensors. pH control was not introduced, hence the medium contained phosphate buffer. Dimensions of the reactor can be found in the Appendix 5.

Appendix 5 Table 7 Conditions of the experimental batch run of *C. necator* Δpha.

Aerobic Batch run	
<b>Gas composition in the headspace</b>	CO <sub>2</sub> 10 %, H <sub>2</sub> 4 %, air 86 %
<b>Initial pressure (atm)</b>	1
<b>Temperature (°C)</b>	28
<b>pH</b>	7
<b>Stirrer speed (rpm)</b>	900
<b>Base control</b>	no
<b>Working volume (ml)</b>	400
<b>Headspace volume (ml)</b>	10850 (0,85 L reactor + 10 L airbag)
<b>Medium</b>	JMM

### 3.3.3. Microorganism cultivation

*C. necator* Δpha retrieved from the cryostock was used in the experiment. Starter culture was grown on JMM medium supplemented with fructose (20 g/L). For cultivation, JMM medium with NH<sub>4</sub>Cl as the only nitrogen source was chosen. The reactor was inoculated with 10 ml starter culture, which prior to inoculation was centrifuged and resuspended in fresh medium. Along with the inoculum, sterilised solution B of JMM medium and vitamins were administered through the feed inlet.

### 3.3.4. Sampling

Samples were collected in the vials installed in a sampling port. Sampling was performed by creating a vacuum in the headspace using a syringe attached to a filter, causing the fluid flow into the vial. Each vial was autoclaved and sprayed with 70 % IPA at exchange. Overall, 10 samples of 10 ml were taken over 4 days. The samples were used for CDW measurement. Additionally, the remaining liquid of an initial and end point sample was used for the analyses including TOC/TN, NO<sub>3</sub><sup>-</sup>, NH<sub>4</sub><sup>+</sup> assays and protein content determination. The headspace of reactor and the gas bag were also sampled with GC syringe.

## 3.4. Measurements

Gas composition was recorded with the GC column as well as the hydrogen sensor continuously gathering data on H<sub>2</sub> concentration in the reactor headspace. Volume of the bag was assessed by inserting it in the box filled with water and weighing. The weight of the box containing fully filled bag and bag at the end of reactor run was measured. The other assays performed are described in the 1st experiment measurements section.

### 3.4.1. Safety measures of reactor cultivation on hydrogen

The following precautions have been taken to maintain safety in the operation of the reactor using hydrogen gas:

1. The hydrogen concentration after filling the reactor headspace could not be higher than 4 %.
2. Hydrogen sensor was inserted in the batch reactor to monitor hydrogen levels and consumption.
3. Hydrogen alarm and sensor were installed in the laboratory. If the level of hydrogen in the room reached 2 %, the alarm would go off. This results in closing the flow of gas between the hydrogen generator and MFC. Additionally, to prevent this situation the hydrogen alarm captures air in the room and burns it at a high temperature.
4. Warning signs with protocols for dealing with alarm activation were displayed on the laboratory door.

## 3.5. Data treatment of the batch experiment

### 3.5.1. Cell growth rate

The growth curve was determined with the Excel's LINEST function, excluding data points which were a result of measurement error. Time and the ln of biomass concentration data points were plotted to find the specific growth rate  $\mu$  (h<sup>-1</sup>), which is expressed in the equations 28 and 29. Biomass concentration was the increment of weight of filter paper divided by the sample volume.

$$\frac{dC_X}{C_X} = \mu dt \quad (28)$$

$$\ln(C_X) = \mu(t_1 - t_0) + \ln(C_{X0}) \quad (29)$$

$C_X$  – biomass concentration  $\left(\frac{g}{L}\right)$

$\mu$  – growth rate  $\left(\frac{1}{h}\right)$

The other data obtained in this experiment were processed in the same way as in already described in the 3.1.4.



## 4. Results

---

This chapter presents the results of the HOB cultivation and liquid culture analyses. The obtained values are the result of several measurement attempts and adjustments of the protocols to match the characteristics of the samples analysed. Applying the aforementioned techniques proved to be a major challenge, as the experimental design was planned from scratch. Cultivation of the bacteria strains has also presented some constraints and challenges, which are addressed in the methodology chapter and further in the discussion part. Moreover, all the results can be accessed via the document in the Appendix 1.

### 4.1. Biomass concentration and cell elemental composition

Optical density recorded at 700 nm during HT24 cultivation showed only the trend of growth. Translating OD740 to OD600 values was inconsistent, as the ratio of the two OD differed between every sample, as seen in the Figure 8.

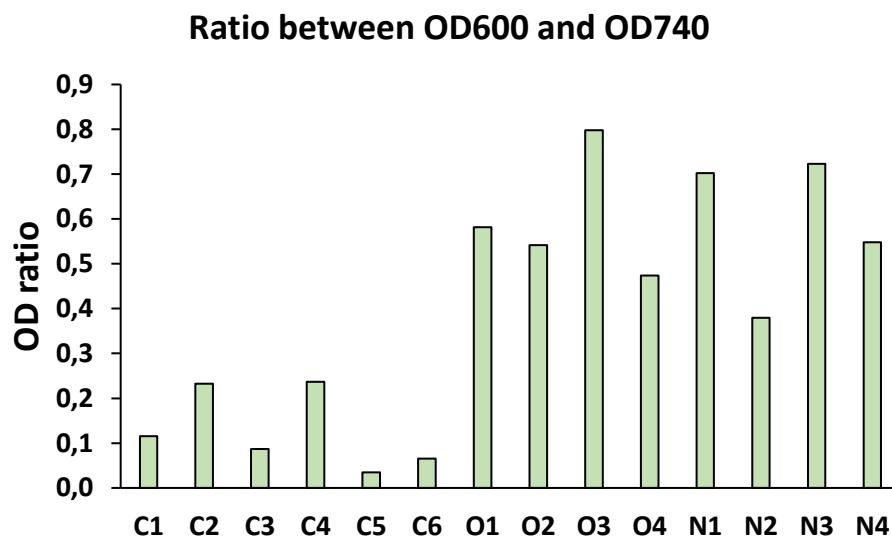


Figure 8 HT24 cultivation run OD740 readings correlated to OD600 (C-control medium sample; O-aerobic condition; N-anaerobic condition).

Slow growth of aerobic samples could be observed on OD740 over time graph but the change in OD for anaerobic samples were almost unnoticeable (Appendix 4). For this reason, *C. necator* run was not done in HT24 but instead in the shaken Kuhner incubator with prepared growth control bottles which were sampled every day, what is shown on the graph below (Figure 8). The aerobic culture started log phase of growth earlier compared to the anaerobic samples, which did not show any significant change in OD.

### C. necator control growth cultures

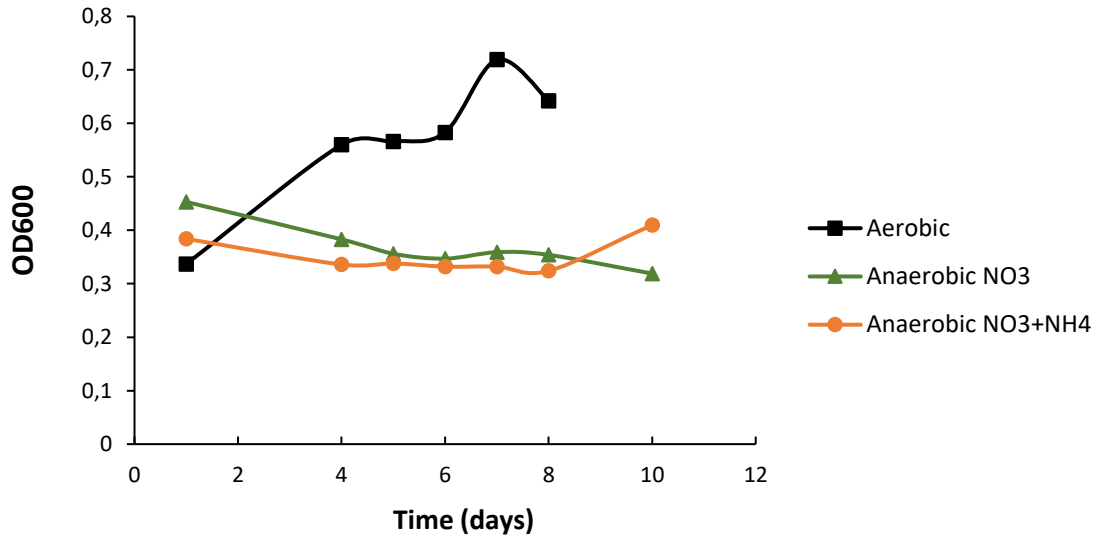


Figure 9 OD600 measurements of control growth samples of *C. necator*.

The average biomass concentration of *C. necator* was determined in two ways. The first approach included the direct CDW measurement carried out on filter papers (Figure 10). According to this dataset, no biomass gain was found in the aerobic cultivation, giving the negative filter weight difference. On the other hand, the anaerobic cultures have grown up to  $0.13 \pm 0.11$  g/L and  $0.14 \pm 0.088$  g/L. However, standard deviation values are above 60% of these values, which demonstrates the wide variability of the data.

### Biomass concentration based on the dry cell weight

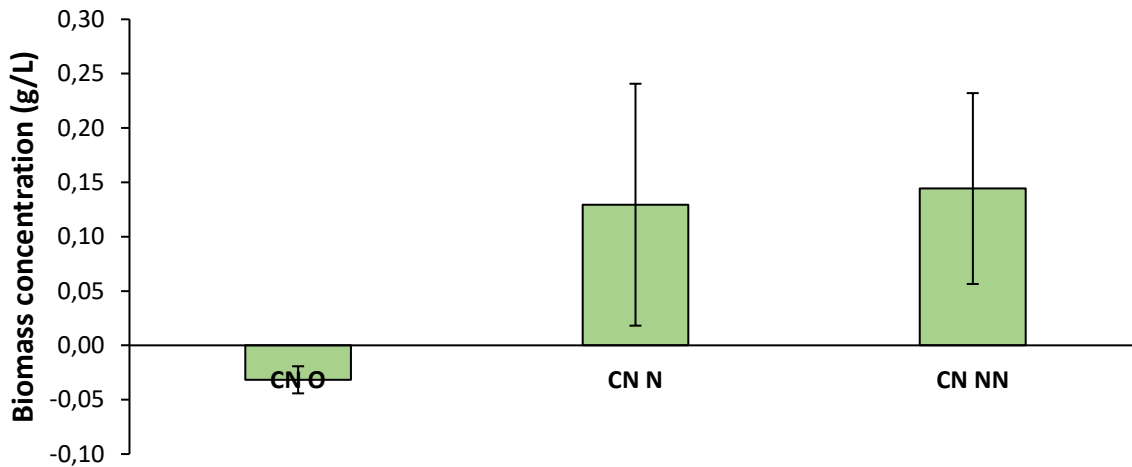


Figure 10 Biomass concentration based on cell filter-drying assay of *C. necator* cultivated in aerobic and anaerobic conditions (CN – *C. necator*; O- aerobic culture; N- anaerobic culture with nitrate; NN- anaerobic culture with nitrate and ammonium).

In contrast to the data presented above, *C. necator* shows the opposite growth behaviour, as presented in the Figure 11. Aerobic culture has reached  $0.143 \pm 0.006$  g/L, whereas the negative concentration values of anaerobic cultures indicate inability of growth. The negative value instead of 0 may be a result of biomass degradation, thus final amount of biomass is lower than after

inoculation. In all the cases, the deviation of concentration values is lower than in the filter-drying determination method.

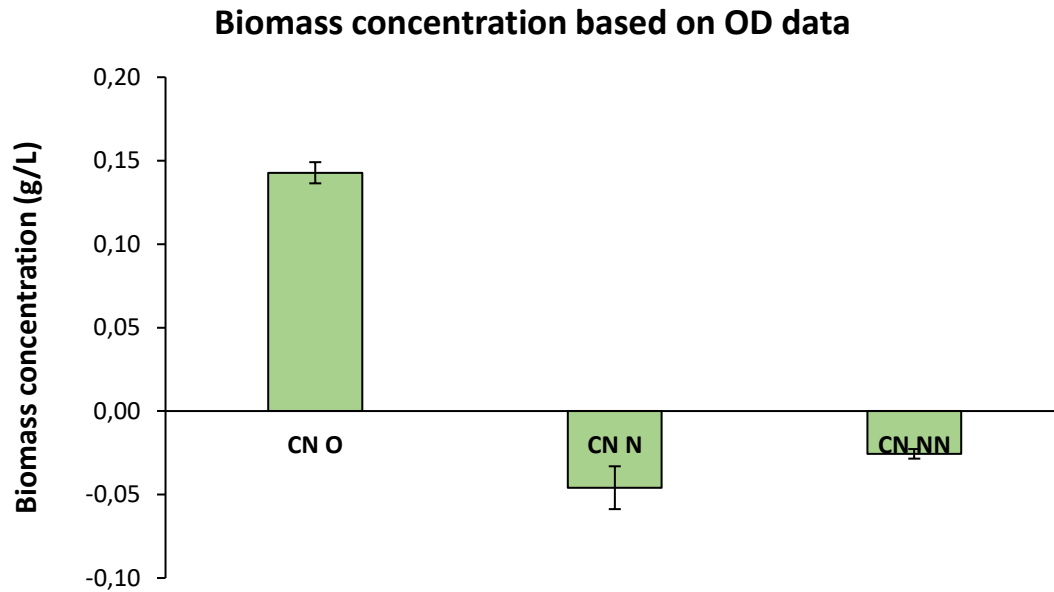


Figure 11 Biomass concentration calculated from CDW/OD curve of *C. necator* cultivated in aerobic and anaerobic conditions (CN – *C. necator*; O- aerobic culture; N- anaerobic culture with nitrate; NN- anaerobic culture with nitrate and ammonium).

Moving on to the other HOB strains, in order to determine the initial concentration of biomass after inoculation, the correlation between OD and CDW had to be established. The curves have not shown a high correlation between OD and CDW of the different biological replicates of a starter cultures (Figure 12). Therefore, the average value of slope and intercept was used to estimate the biomass concentration from OD600 data.

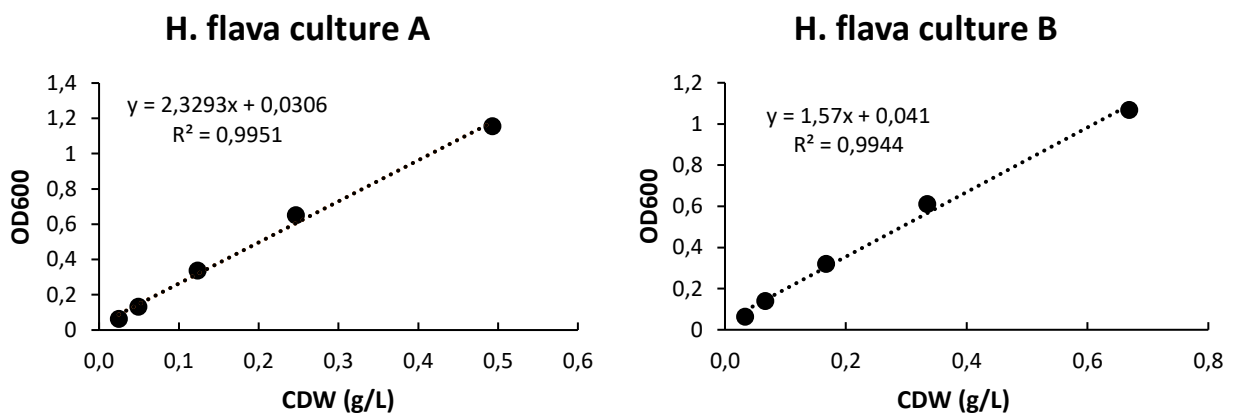


Figure 12 Example of the OD/CDW correlation curves prepared on the biological replicates of *H. flava* starter culture.

### Average biomass concentration (g/L)

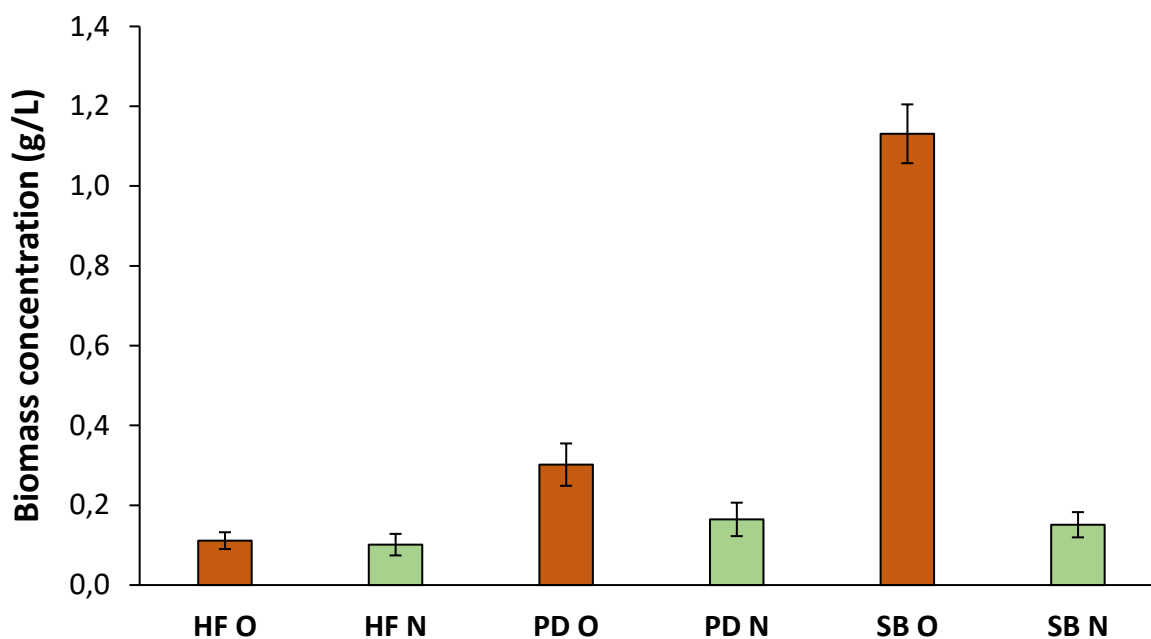


Figure 13 The average biomass concentration of three HOB strains. Letter O indicates aerobic conditions, whereas the N stands for anaerobic cultivation (HF- *F. flava*; PD - *P. denitrificans*; SB - *S. barnesii*).

The increment of biomass in aerobic conditions is higher than in the anaerobic cultures for every examined strain (Figure 13). Biomass concentration of *S. barnesii* aerobic culture reached  $1.3 \pm 0.074$  g/L making it the best performing bacteria. HOB respirating on nitrate between 0.1 and 0.16 g/L, showing similar growth pattern.

#### 4.2. Biomass elemental composition

For the elemental composition determination, TC and TN results were implemented. By using the carbon and nitrogen concentrations in the samples, content of these elements in the biomass samples was determined. The discrepancy between the results of individual biological replicates as well as between strains appears to be very noticeable.

In the first attempt of TC determination, the given values of supernatant carbon exceeded its content in the broth. Therefore, the mean concentration values of TC in the broth given by the analyser software were adjusted and compared with the other dataset. The adjustment yielded positive carbon concentrations which were afterwards compared to biomass concentrations data from the OD and filter-drying analyses.

The 1<sup>st</sup> data set show several results with a decrease in carbon content of the sample where biomass growth occurred based on the biomass concentration assays (Figure 13). Furthermore, for samples with carbon increase over the biomass growth, the amount of gained carbon does not correspond to the typical mass fraction (approximately 48 %) of this element in the dry biomass [62]. Whereas the 2<sup>nd</sup> dataset provides the information that there is increase of biomass in every strain with a recorded biomass increment. The mass fraction of carbon in the biomass reached between 40 and 50 % for anaerobic *H. flava*, *P. denitrificans* and aerobic *C. necator* samples. At the same time, carbon content exceeded 100 % of biomass weight in aerobic *H. flava* and anaerobic *S. barnesii* samples. Even though, several samples have the carbon content in the expected range, inconsistency makes reliability of the data debatable.

It is worth mentioning that *S. barnesii* samples have shown 4-10 times higher initial and final carbon concentration compared to other strains due to the presence of CAPS buffer in media consisting of an organic carbon. Moreover, the large changes of carbon both positive and negative were recorded

for control media samples, where in principle the biomass was not present. This indicates contamination or large measurement error.

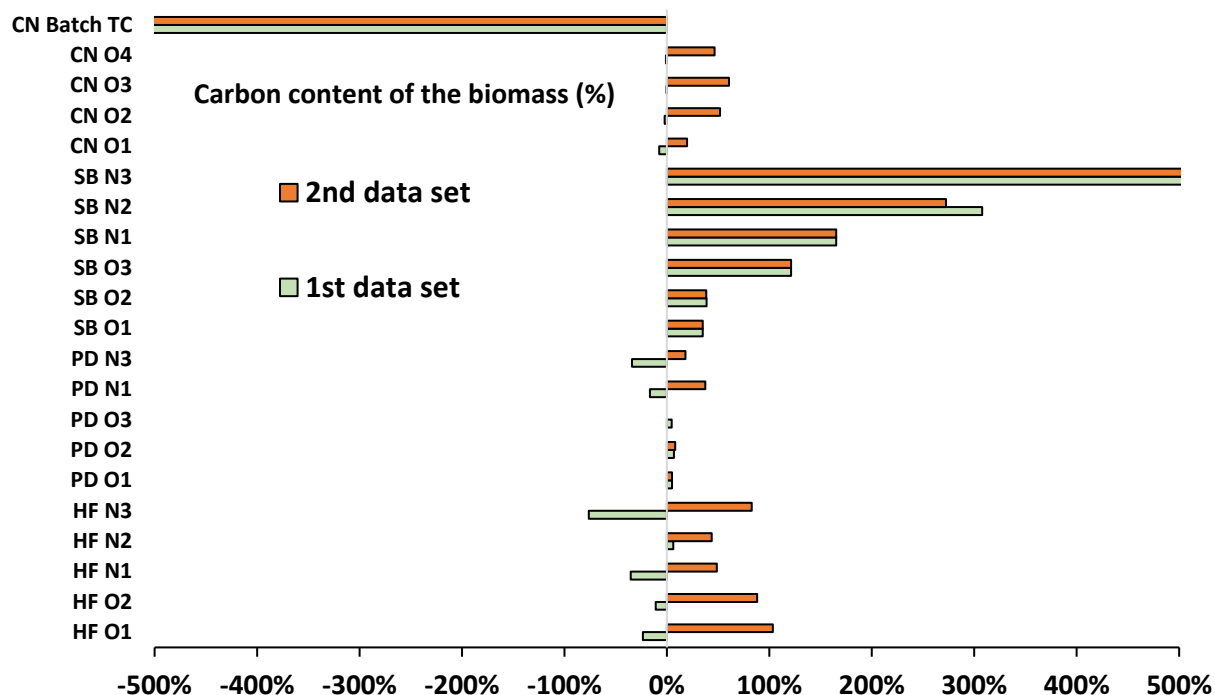


Figure 14 Comparison of the total carbon content of the biomass in the examined HOB samples. Total carbon change is not presented for the samples with no increment of the biomass (HF-*H. flava*; PD-*P. denitrificans*; SB-*S. barnesii*; CN-*C. necator*; O-aerobic; N- anaerobic).

The molar content of elemental carbon, which was calculated separately for the initial and final biomass CDW is presented in Table 8. The results of aerobic and anaerobic samples have wide variance, showing more than 2 moles of carbon per mole biomass what makes it very unlikely to be a true value. As the broth culture was not investigated in TN assay and  $\Delta$ TN over biomass growth increase did not provide reliable data, the elemental composition of nitrogen could not be established.

Table 8 The elemental carbon composition of the HOB cell.

HOB	HF O	HF N	PD O	PD N	SB O	SB N	CN O	Batch
<b>Average molar C content (mol/C mol biomass)</b>	1,455	0,999	0,188	2,341	1,093	4,864	1,129	
<b>Standard deviation</b>	0,07	0,191	0,033	2,152	0,003	0,783	N.A.	

Total nitrogen concentration change over the  $\Delta$ CDW presents two patterns. *P. denitrificans* and aerobic *C. necator* samples contain 2-10% and 10-13% of nitrogen by weight, which is lower than the expected 14%, although the uncertain biomass concentration data could contribute to the error. Other samples present the negative change of nitrogen concentration, indicating the increase of nitrogen compounds in the supernatant. Moreover, the expected initial values based on the nitrogen concentration in the prepared cultivation media were not reached. TN results are not in accordance with the nitrogen concentration data obtained from  $\text{NO}_3$  and  $\text{NH}_4$  analyses, giving 2-3 times less nitrogen.

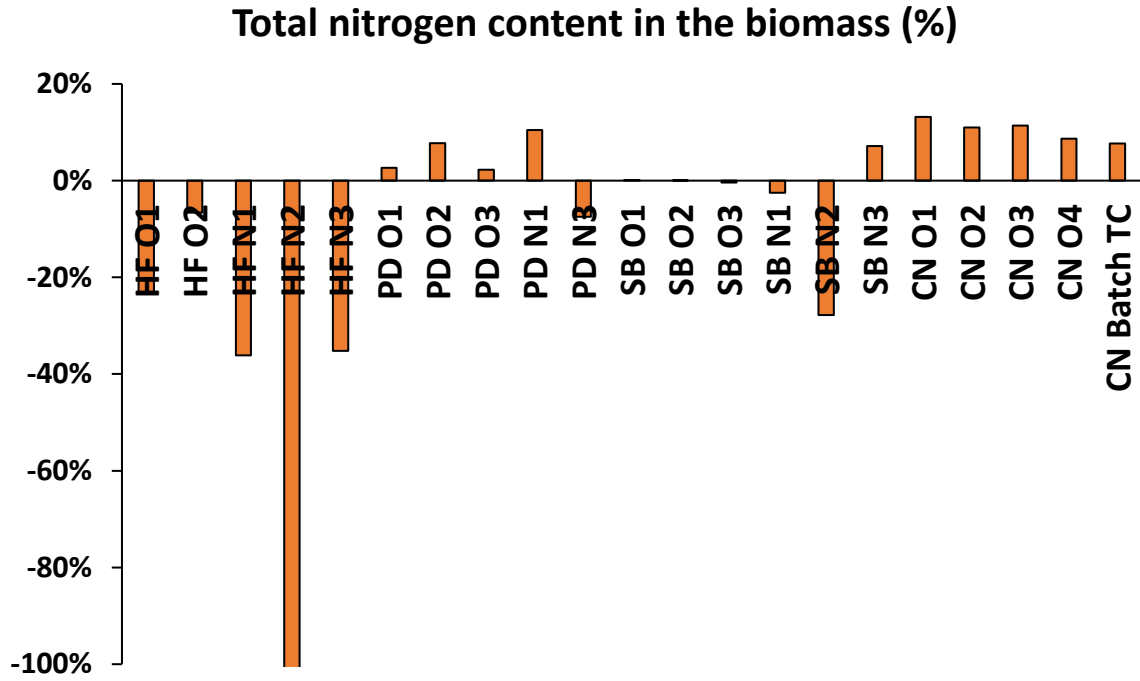


Figure 15 Comparison of the total nitrogen content of the biomass in the investigated HOB strains (HF-*H. flava*; PD- *P. denitrificans*; SB-*S. barnesii*; CN-*C. necator*; O-aerobic; N- anaerobic).

To sum up, cell elemental composition of carbon and nitrogen could not be determined as the results were burdened by the unreliable biomass concentration results along with the distorted TC and TN readings.

### 4.3. Gaseous substrates consumption

The molar oxygen consumption over the initial gas content has provided the consumption efficiency. In case of *C. necator*, *H. flava* and *P. denitrificans* the average consumption of oxygen was around  $80 \pm 5\%$ . *S. barnesii* has utilized only  $26 \pm 2.7\%$  total available oxygen (Figure 16). The decrease of initial oxygen content was also recorded in the control media samples, what could be caused by the gas leakage or gas transfer to the liquid. In the several individual samples oxygen was found to be higher than initially.

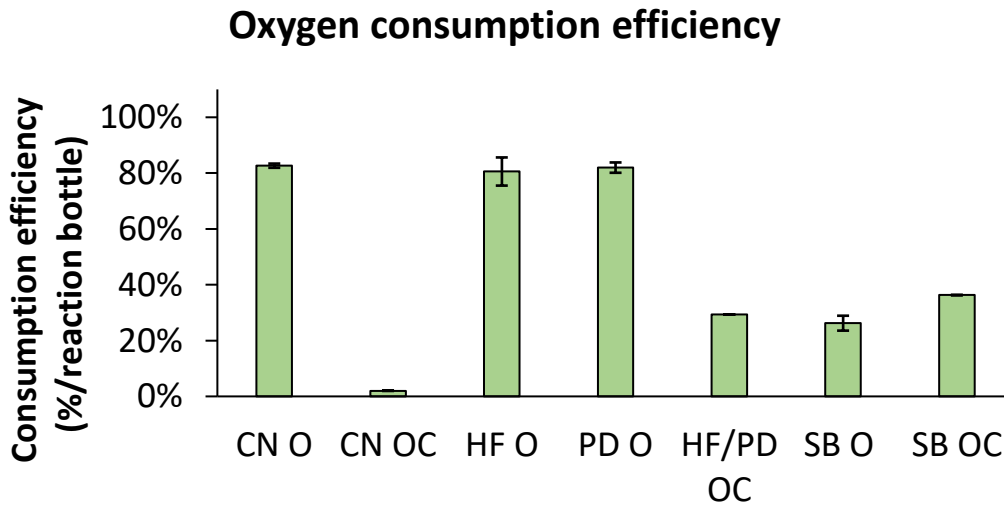


Figure 16 The efficiency of oxygen consumption shown for the HOB cultivated aerobically (CN-*C. necator*; HF-*H. flava*; PD-*P. denitrificans*; SB-*S. barnesii*; O-aerobic sample; OC- aerobic control).

Contrary to the expected lack of change in the nitrogen molar content for the aerobic cultivation, or an increase due to the denitrification, the gas was consumed. The average dinitrogen consumption was between 10 and 30 % of the total initial content, as presented in the Figure 17. *C. necator* exhibited the largest standard deviation along with the aerobic *H. flava* due to wide discrepancy in the results. However, the control media samples of *C. necator* did not note N<sub>2</sub> decrease.

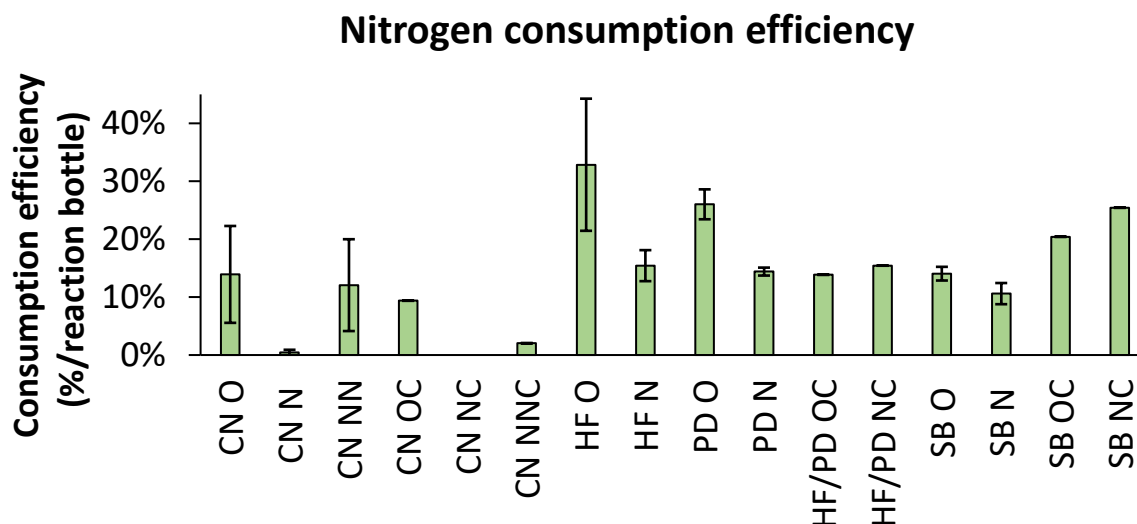


Figure 17 The efficiency of nitrogen consumption shown for the HOB cultivated aerobically (O) and anaerobically (N/NN) (CN-*C. necator*; HF-*H. flava*; PD-*P. denitrificans*; SB-*S. barnesii*; OC-aerobic control; NC/NNC-anaerobic control).

Electron donor was almost entirely consumed by the aerobically cultivated strains, except *S. barnesii* (Figure 18). Bacteria cultivated in anaerobic condition had reached lower biomass concentration, therefore a smaller hydrogen fraction was consumed. Considering the measured biomass increment, *S. barnesii* seem to have grown without hydrogen, which raises the question of how this HOB culture could have grown autotrophically. Moreover, some hydrogen was consumed even in the experimental bottles where no biomass was formed e.g., media control of *C. necator*.

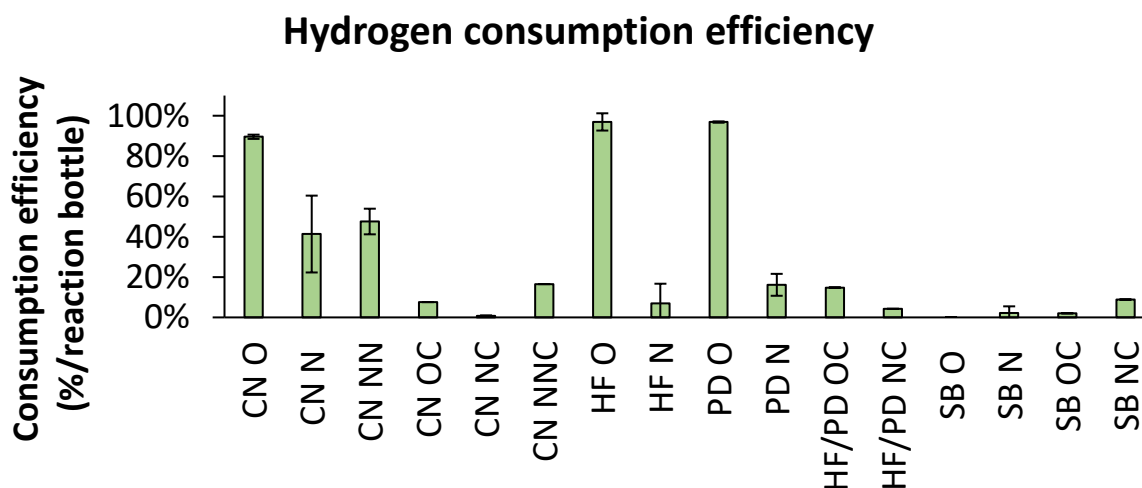


Figure 18 The efficiency of hydrogen consumption shown for the HOB cultivated aerobically (O) and anaerobically (N/NN) (CN-*C. necator*; HF-*H. flava*; PD-*P. denitrificans*; SB-*S. barnesii*; OC-aerobic control; NC/NNC-anaerobic control).

#### 4.4. Nitrate yield

The nitrate concentration change over the cultivation period was measured to estimate the efficiency of the anaerobic respiration as well as to complete the biomass formation equation with the NO<sub>3</sub><sup>-</sup> consumption rate. The initial NO<sub>3</sub><sup>-</sup> concentration was equal 7.2 ± 1 g/L which suited the expected concentration range based on the 6.8 g/L nitrate in the prepared media.

The electron acceptor yielded  $0.49 \pm 0.3$  mol of  $\text{NO}_3^-$  per 1 mol BM in the first biological replicate, whereas the second reached  $3.02 \pm 2.01$  mol  $\text{NO}_3^-$ /mol BM, thus regarding wide standard deviation these values are not very accurate (Figure 19). In case the yield is shown as 0, either nitrate concentration increased over time, or the biomass did not show any growth.

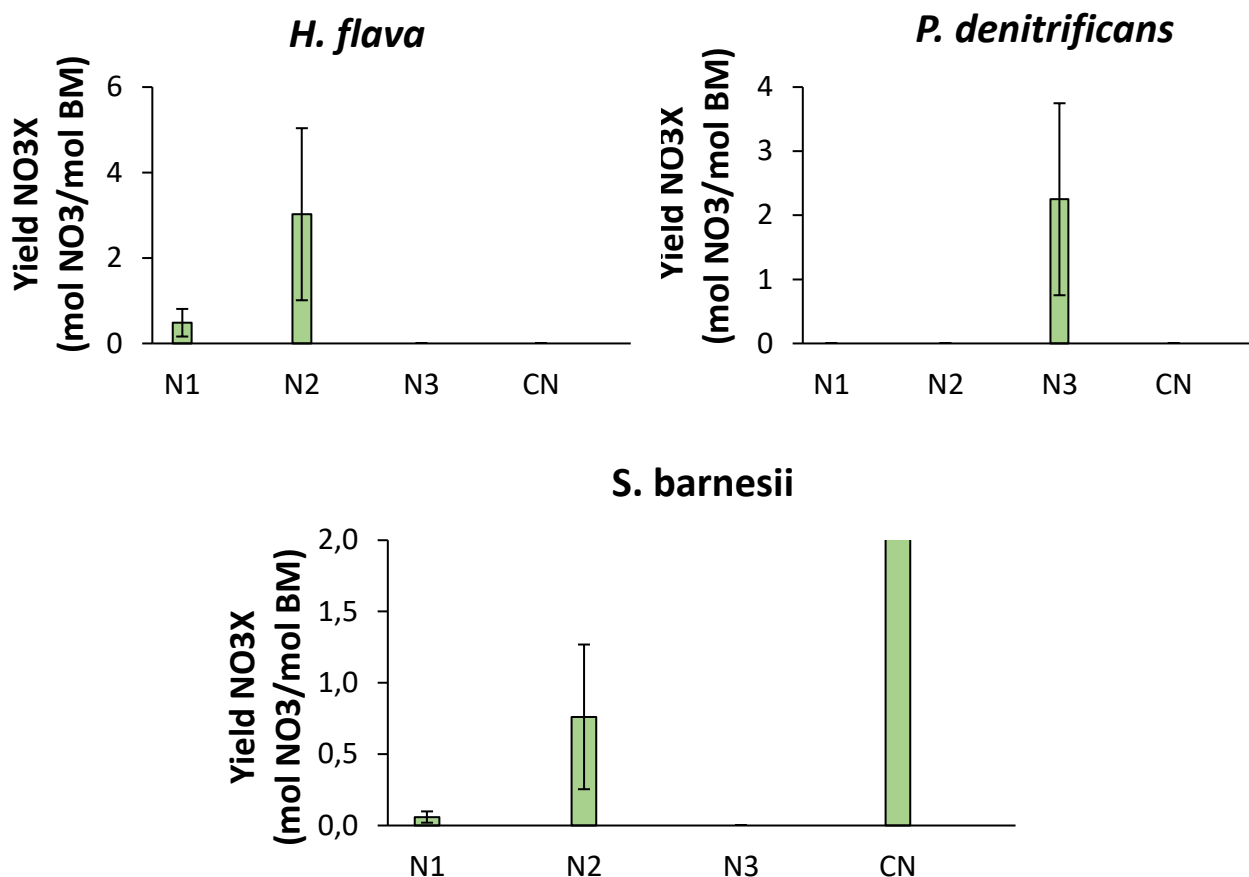


Figure 19 Nitrate yield on the biomass of the anaerobic *H. flava*, *P. denitrificans* and *S. barnesii* samples (CN-control media; N-anaerobic sample replicate).

The similar case applies to the other strains. Only 3<sup>rd</sup> anaerobic replicate of *P. denitrificans* gave  $2.25 \pm 1.5$  mol  $\text{NO}_3$ /mol BM, as other samples showed the production of nitrate. *S. barnesii* first replicate noted low yield of  $0.06 \pm 0.04$  mol  $\text{NO}_3$ /mol BM. The second replicate had a higher yield reaching  $0.76 \pm 0.5$  mol  $\text{NO}_3$ /mol BM. Additionally the control medium sample had given  $371.15 \pm 247.11$  mol  $\text{NO}_3$ /mol BM, which is likely caused by the measurement error of the end point sample. The standard deviation indicates high inaccuracy of the obtained results.

Furthermore, *C. necator* anaerobic samples haven't achieved biomass gain thus the yield could not be calculated.

#### 4.5. Ammonium yield

The ammonium change of concentration was measured to indicate the biomass growth, identify the DNRA process if it occurred and calculate how much  $\text{NH}_4^+$  could be used in the Ostwald process. It needs to be addressed that even though ammonium chloride was not added to the anaerobic media, except a *C. necator* anaerobic NN set, very low concentrations were detected. It could be caused by the presence of ferric ammonium citrate in HF and PD medium as well as minimal amounts being the product of nitrate reduction with resazurin. An initial  $\text{NH}_4^+$  concentration was on average  $310.23 \pm 63.9$  mg/L which was in accordance with the 0.3 g/L ammonium added to the medium.

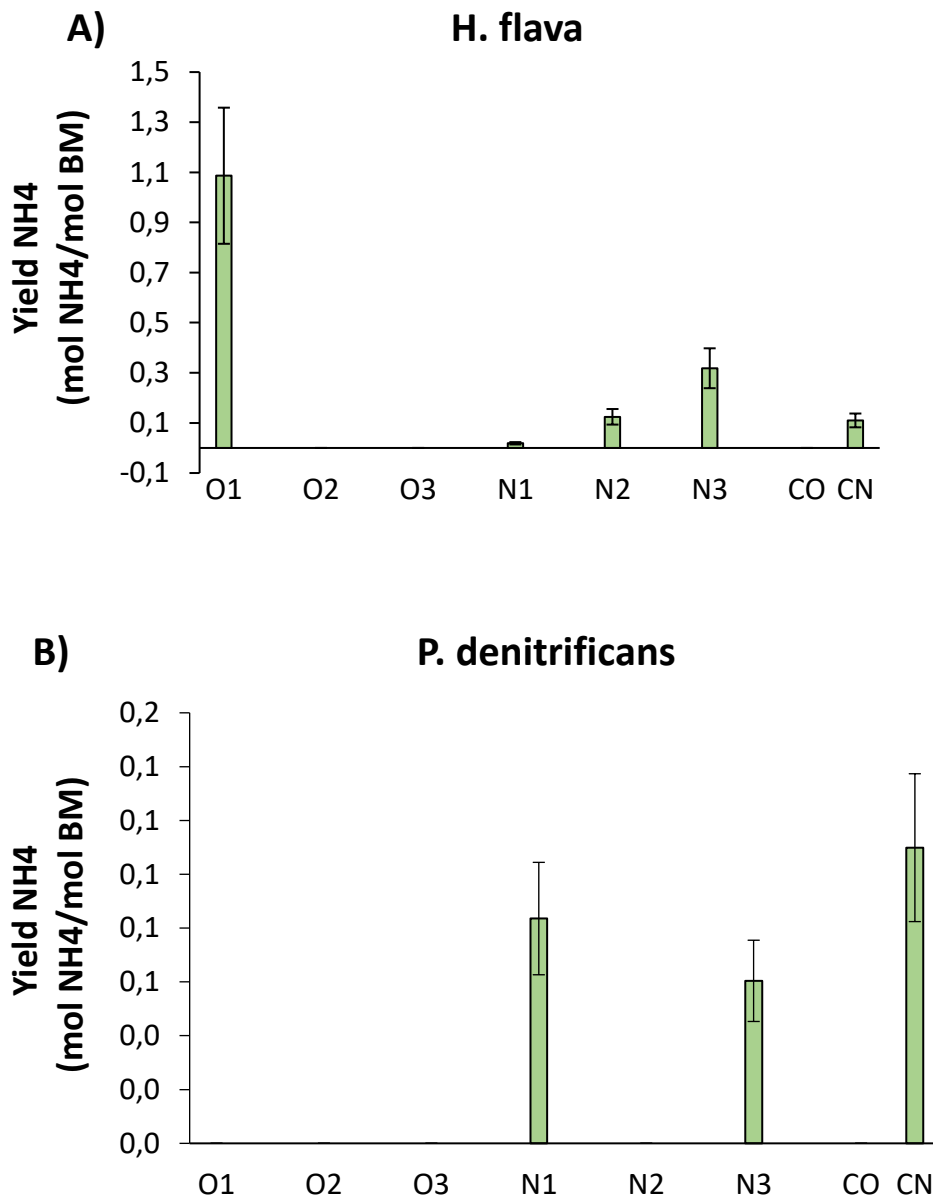
Ammonium was consumed in only one replicate of aerobic *H. flava* culture (Figure 20.A). The 0 value of the second and third replicate are linked with no biomass increment of HF O3 and increase in ammonium value by 70 % in HF O2. The increase is most likely caused by the error done during



addition of too much assay reagents to the sample. In the anaerobic samples low ammonia concentrations were consumed giving yields of  $\text{NH}_4^+$  on biomass comparably lower than in the aerobic cultures.

In aerobic *P. denitrificans* samples the increase of around 50 % of the initial ammonium was noted, thus the yield of substrate  $\text{NH}_4^+$  on biomass could not be obtained (Figure 20.B). Moreover, low consumption occurred in two anaerobic samples as well as low increase in  $\text{N}_2$ . As the yields do not exceed 0.08 mol  $\text{NH}_4^+$  /mol BM and the results are subject to an error of 0.02 mol  $\text{NH}_4^+$  /mol BM, that the PN  $\text{N}_2$  sample can be incorrectly measured as an increment. Furthermore, the increase of ammonium in the control medium CN in which the concentration should have not changed, indicates contamination or measurement inconsistency.

*C. necator* has given a positive ammonium yield on the biomass in case of aerobic samples (Figure 20.C). The standard error of the yield calculation did not exceed 25 %, thus the results appear to be quite reliable. Even though high consumption was also found in the anaerobic samples containing ammonium, there was no growth of the biomass, thus the yield could not be calculated. The decrease of ammonium would indicate nitrogen assimilation, which does not agree with the CDW concentration measurements. Moreover, in the *C. necator* batch experiment ammonia the yield of  $0.66 \pm 0.16$  mol  $\text{NH}_4^+$  /mol BM was recorded. This is supported by biomass increment of 0.25 g/L.



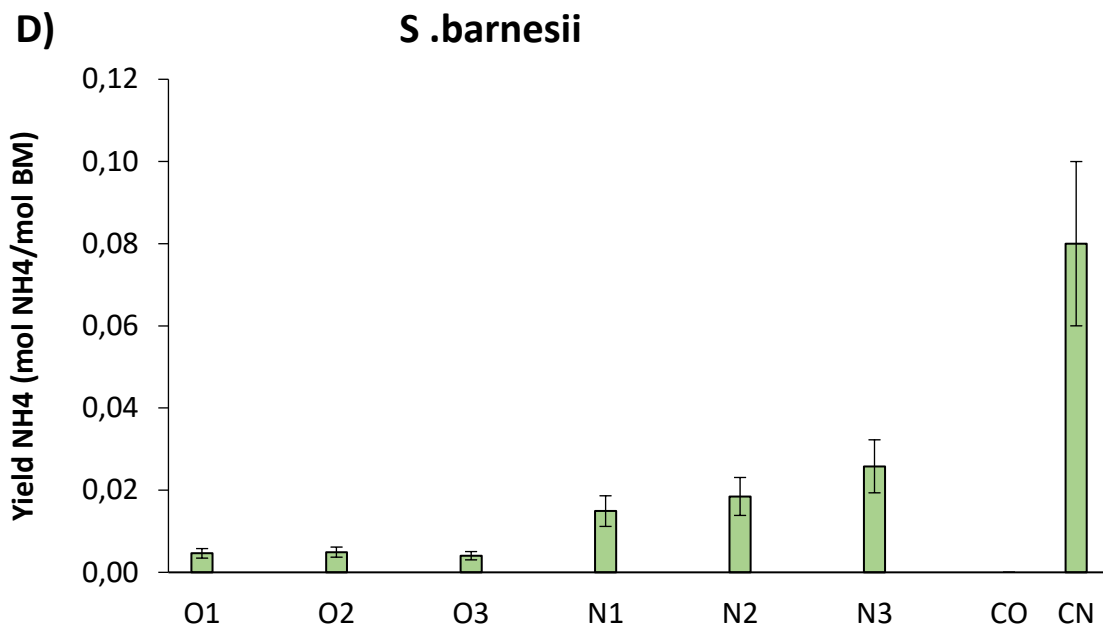
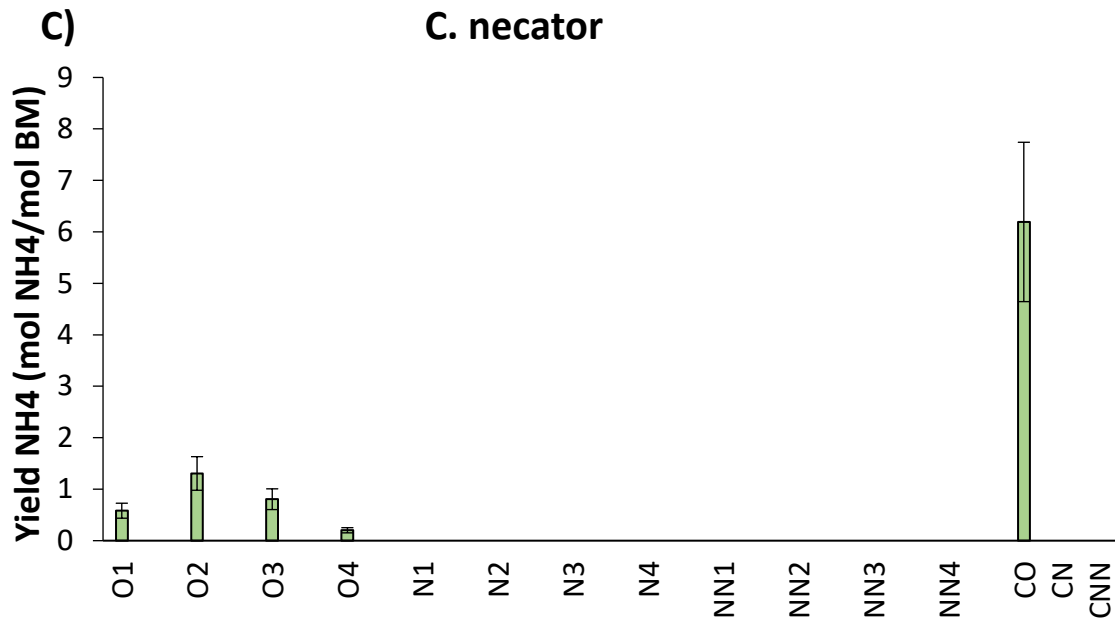


Figure 20 A.B.C.D Yield of  $\text{NH}_4^+$  on the biomass of the *H. flava*, *C. necator*, *P. denitrificans* and *S. barnesii* samples (CO- aerobic medium control; CN/CNN- anaerobic medium control; O- aerobic replicate; N- anaerobic replicate).

Regarding low initial concentration of ammonium in the medium, *S. barnesii* presents negative concentrations both for the initial and end point measurements. The calculations are based on the standard curve with a range from 0 to 100 mg  $\text{NH}_4\text{-N}$ , suggesting that the actual concentration in the medium was lower than expected 27 mg/L ammonium or the standard loses accuracy when reaching the lower limit. Nevertheless, the final ammonium concentration was lower than the initial, thus consumption occurred and the yields on the biomass could be obtained (Figure 20.D).

Looking at the Figure 21, in *H. flava* and *P. denitrificans* aerobic samples, a production yield of ammonium was determined. This data is contradictory to the aerobic culture behaviour, as the ammonium should be assimilated into growing biomass. Standard error is 25 %, being not sufficiently big to allow rejection of the results. These data will be discussed in the following chapter.

## Production Yield NH<sub>4</sub> on biomass

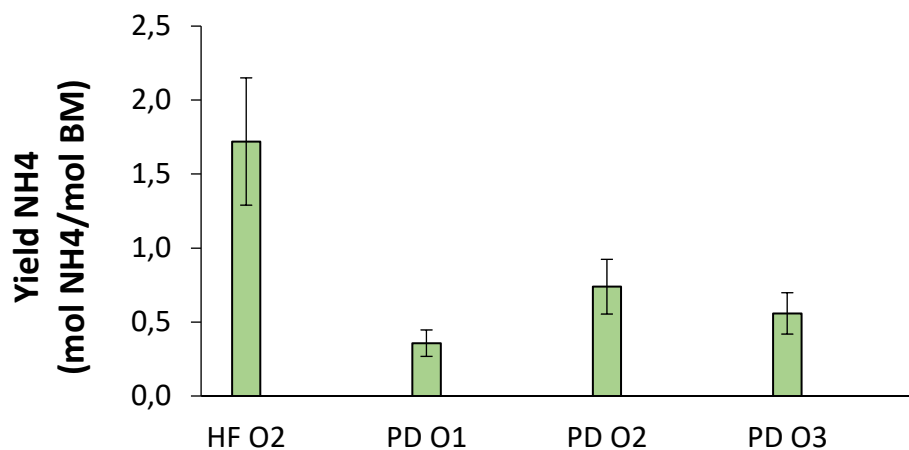


Figure 21 Production yield of ammonium on the biomass for HOB strains (HF- *H. flava*; PD - *P. denitrificans*; O- aerobic culture replicate).

### 4.6. Protein content of the biomass

The standard calibration curve has given a correlation coefficient of 0.999 and it ranged from 0 to 100 mg/L BSA, thus it was well adjusted to low protein concentrations. The calculated protein concentration is an average of the results obtained from the triplicates. Standard deviation below 10 %, supports accuracy of OD measurements.

According to Table 9, majority of the results show the protein content in the cell above 100 % of its weight. These amounts are not biologically possible, making the data unreliable. In every examined strain, individual samples have reached reasonable protein contents e.g.,  $53.3 \pm 0.4$  % for *S. barnesii*,  $58.4 \pm 3.5$  % for *C. necator* and  $82.2 \pm 2.6$  % for *P. denitrificans* culture. However, considering the inconsistency of obtained results within one strain, these outcomes cannot be validated.

Furthermore, the tendency of protein content can be observed between aerobic and anaerobic samples. In *H. flava* and *S. barnesii* anaerobic samples, less protein is noted, whereas higher protein content applies to *C. necator* and *P. denitrificans* anaerobic cultures. However, different respiration mode should not affect the protein content so significantly, thus this observation is burdened by the inconsistency of all the results.

Table 9 Protein content of the HOB strains. (HF-*H. flava*; PD-*P. denitrificans*; SB- *S. barnesii*; CN-*C. necator*; O-aerobic; N- anaerobic).

Sample	Protein concentration (g/L)	BM concentration (g/L)	Protein content (%)	Standard deviation
HF_O2	0.336	0.187	179.6%	5.2%
HF_N1	0.239	0.223	107.3%	2.4%
HF_N2	0.284	0.203	139.9%	9.2%
PD_O1	0.333	0.405	<b>82.2%</b>	2.6%
PD_O3	0.491	0.315	156.0%	2.8%
PD_N1	0.469	0.253	185.5%	4.2%
SB_O1	0.838	1.180	<b>71.0%</b>	6.9%
SB_O2	0.659	1.235	<b>53.3%</b>	0.4%
SB_N1	0.039	0.262	15.0%	1.8%
CN_O2	0.392	0.264	148.6%	7.2%
CN_O3	0.395	0.255	155.3%	1.1%
CN_N1	0.268	0.138	194.3%	6.7%
CN_Batch	0.217	0.371	<b>58.4%</b>	3.5%

#### 4.7. Biomass formation equation and energy cost

The data obtained in the previous analyses were used to fill in the biomass formation equation with the molar rates of substrates consumed and products generated over the cultivation time. Balancing the equation with water molecules and protons was done. Moreover, the stoichiometric coefficient of the biomass equation was applied to calculate the yield of hydrogen on the biomass and the enthalpy of reaction.

Due to the fact that most of the results were burdened with high inconsistency and lacking reliability, it was not possible to obtain realistic values that would be comparable between replicates of a given strain. Therefore, the stoichiometry, yields and enthalpies are not valid and cannot be compared with the literature data. Determination of the most energetically efficient HOB has not succeeded.

#### 4.8. Batch reactor experiment

#### 4.9. Growth rate of *C. necator*

The batch experiment was completed after 93 hours, through which the broth samples were taken to determine biomass concentration using the filter-drying method. The results of measurements are presented in Figure 22. Only 11 samples were taken because of the low broth volume limited by the reactor gas headspace. Flocs were present in the initial sample which overstated the biomass concentration result, thus the data from the next sample was used as an initial plot point. Two other results were rejected due to overestimation caused by contamination in the sampling bottle.

The growth plot has too few data points to identify clearly what the growth behaviour of *C. necator* looks like. From the obtained data points linear growth, ending with less steep curve is shown. The lag phase followed by the log and stationary phase is not observed. Plotting natural logarithm of biomass concentration datapoints against time given a linear slope (Figure 23). Based only on the available data maximum growth rate could not be calculated. However, the average growth rate ( $\mu$ ) over the experimental period of growth was determined, being equal to 0.021 (1/h).

### C. necator growth over time

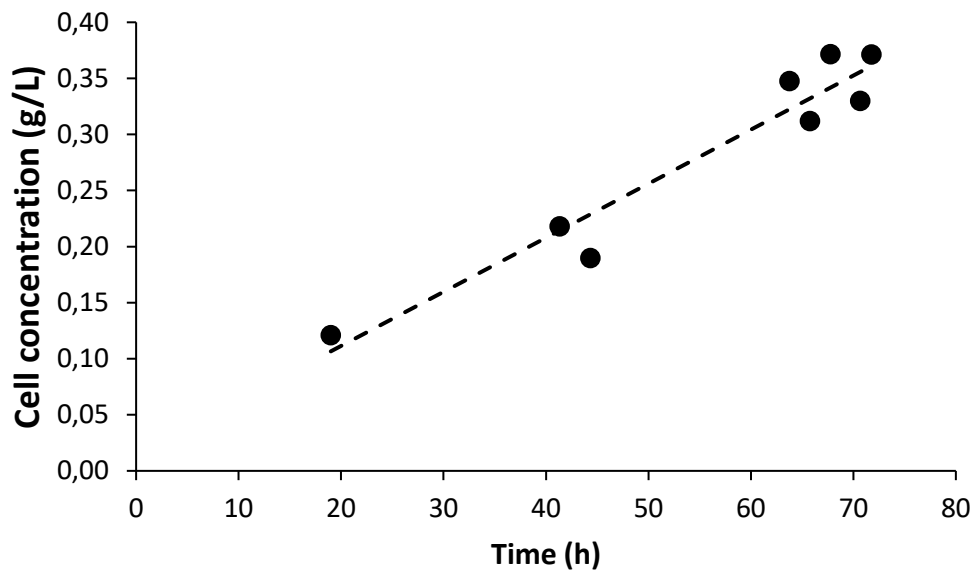


Figure 22 *C. necator* growth over time during aerobic cultivation in the batch reactor.

### C. necator growth rate

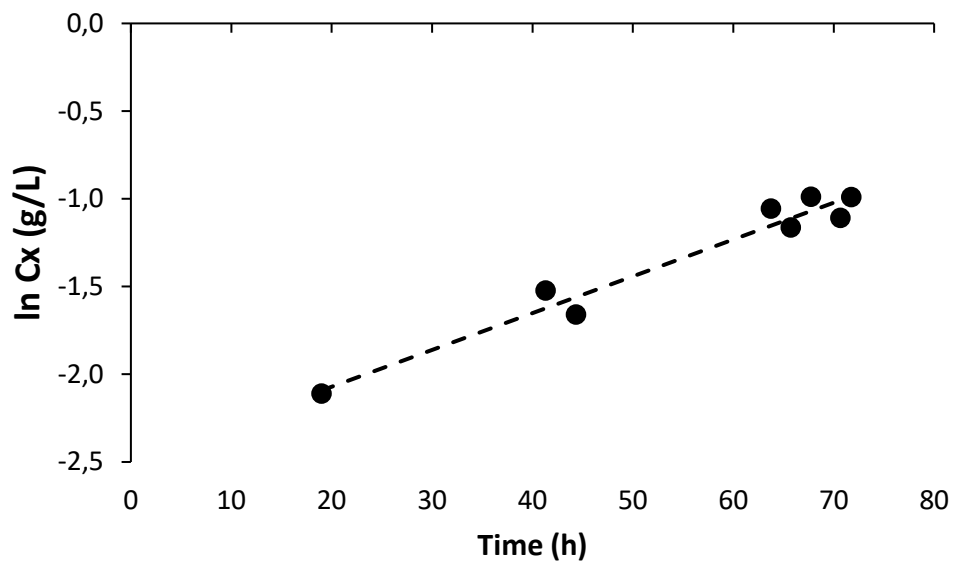


Figure 23 Determination of the aerobic *C. necator* culture growth rate.

## 5. Discussion and recommendations

---

This chapter is focused on the evaluation of the quality of experimental design and reliability of measurement methods and results. Moreover, the improvement of the experimental setup is suggested including adjustments of the established protocols and recommendations to implement new methods of measurements.

### 5.1. Biomass concentration

Regarding the use of HT24 for continuous OD measurements, the outcome data was found to be not particularly useful. The serum bottles were not suitable for optical density measurements as their glass walls were irregular, causing alterations in the obtained OD values. Moreover, any movement of the bottle would change the reading as well. Therefore, it is proposed not to use the HT24 reactor for cultivation, as the gastight serum bottles do not suit the specifications of the device. Carrying out the experiment in the Kuhner incubator with growth control samples seem to work sufficiently, as the growth plots can be updated every sampling.

The biomass concentrations presented in Figure 11 and Figure 13 were measured in the aerobic and anaerobic cultures harvested at the same time. Therefore, the bacteria cultivated with nitrate as an electron acceptor show slower growth. This behaviour is supported by the study on growth of HOB via denitrification and DNRA. As a result of less amount of energy released and converted into ATP during respiration, bacterial growth is hindered [26]. It was found that the anaerobic autohydrogenotrophic growth was reduced by 90-95 % in *C. necator* in comparison to its aerobic cultivation [52]. Additionally, the decrease of growth yield on hydrogen by half was noted in *P. denitrificans* culture cultivated under denitrifying conditions [63].

When it comes to reliability of the biomass concentration results, the issue occurs both with the OD based and filter-drying determined data. Difference between results in Figure 10 and Figure 11 show how completely opposite values can be obtained through these two methods. Although, the OD based calculations appear to present more realistic growth behaviour due to the increase of the biomass in aerobic cultures opposed over 10 days opposed to the anaerobic samples.

For the OD based approach, a calibration curve was prepared using the stater culture grown heterotrophically. Consequently, the growth behaviour and cell size can differ in the autotrophically grown HOB. Variation in the correlation of OD to CDW depending on cultivation conditions can be observed on the example of *C. necator*. In this work 1 OD translated to 0.39 g/L biomass, whereas other study on hydrogenotrophic cultivation obtained 0.25 g/L at 1 OD [51]. In the study cultivating *C. necator* at the heterotrophic hydrogen respiring conditions, the biomass reached 0.45 g/L at 1 OD. Either determination of CDW/OD curves in the same cultivation conditions or directly measuring CDW of initial and final biomass samples is a solution that would allow to obtain more accurate data.

Regarding the biomass filtration method, the filters with 0.7  $\mu\text{m}$  pore size were used. The recommended pore sizes of filter for bacteria filtration are 0.45 and 0.22  $\mu\text{m}$ , thus it was possible that some biomass passed through the filter paper [64]. Moreover, salt sediments from medium along with contaminant flocks were filtered along with the biomass. Using the filter papers of smaller pore size should improve the filter-drying protocol. Furthermore, performing centrifugation and discarding supernatant, then resuspending the pellet to remove any interference from medium compounds is strongly recommended before applying filter-drying method.

The negative values of the biomass concentration of anaerobic cultures in Figure 11 could be explained by the lower OD readings in the harvest samples compared to the initial as a result of cells lysis over the cultivation period. On the other hand, the results are burdened with the error of the OD/CDW correlation curve and filtration method, thus the cells may have had not started growing yet, remaining in the lag phase. Prolonged lag phase could cause that the experiment was finished before bacteria started to grow exponentially, thus the cultivation time was too short. The suggestion for estimation of growth time is to run a test culture in anaerobic condition with nitrate at least 2 weeks, as there was no OD increase in *C. necator* run after 10 days. However, the medium

composition could also be the issue as it was a medium recommended by DSMZ at particular conditions, usually aerobic. Changing only the nitrogen source could still not provide the most suitable conditions for anaerobic cultivation. Further research on adapting the medium for anaerobic growth and optimal time of cultivation is recommended to ensure a successful experiment.

## 5.2. Carbon content of the cell

Initially, TC and TN of the supernatant were measured using one analytic method which sets the calibration curve for carbon at 0 -1000 ppm and nitrogen to 0-100 ppm range. This setup does not adjust the calibration curve during replicates measurements, making it more prone to accuracy error. In result the carbon measured with TC/TN method diluted 50 times gave significantly different result than the 10 times diluted total carbon measured only with TC method. For this reason, the results presented in the Figure 14 and Figure 15 are obtained by distinct TC and TN assays. Therefore, it is recommended to carry out TC and TN analysis separately. The molecular biomass formula could not be established as the issue lies in the quality of sample measurements. Regarding Figure 14, two data sets describing the total carbon of examined HOB have provided contradictory results. Thorough investigation of the concentration measurement method has shown discrepancy between the total carbon values of broth and supernatant samples.

Peaks presented in the Figure 24 and Figure 25 of TC show the replicates of a single measurement. Recurrent peak pater can be observed in all the culture broth samples. The first two values are usually between 7-15 mg/L, while the next peaks have the values below 1 mg/L. The device rejects initial data and takes a mean of the low concentrations. Furthermore, the TC peaks of supernatant follow predictable method approach, as the first peak does not exceed the following peaks by ten times. The increased concentration is immediately corrected with the calibration curve, therefore 2nd peak shows almost the same values as in the next replicates. Consequently, the carbon content in the broth is lower than in the supernatant. These mean concentrations comprise the 1<sup>st</sup> dataset, which subtracts supernatant TC from the broth values. In order to address this issue, the average of two first datapoints from the broth readings was used for data correction, making the difference between the broth and supernatant carbon more realistic. The 2<sup>nd</sup> dataset reflects the correction of concentrations.

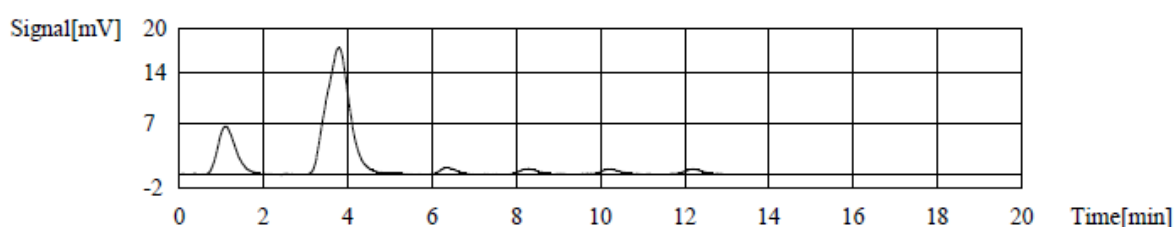


Figure 24 Example of obtained TC peak of culture broth sample.

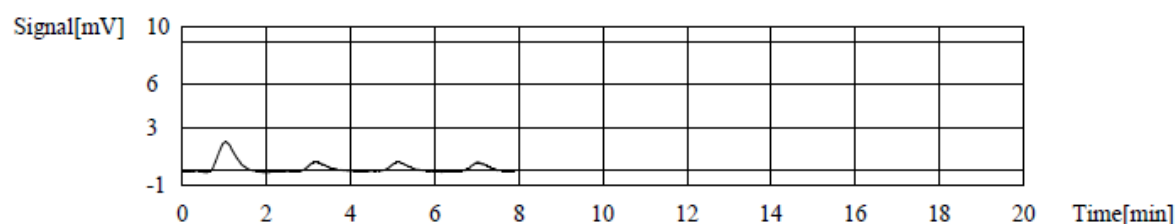


Figure 25 Example of obtained TC peak of culture supernatant sample.

Expected TC values of the culture broth would be significantly higher due to the presence of biomass, whereas supernatant would only contain residual carbon from vitamins, resazurin and the reducing agent if applied. In case of *S. barnesii* cultures TC values were considerably higher than in other HOB strains because of the high concentration of CAPS buffer. Measuring the supernatant carbon allowed to exclude that interfering carbon source from the broth result.

Although, the 2<sup>nd</sup> data set is more in line with the CDW measurements, there are samples in which TC reaches above 100 % of the biomass. In conclusion, the data is still not consistent and therefore

it cannot be considered as reliable. To ensure the quality of TC readings, both the broth and supernatant carbon content must be measured, preferably at the same dilution to decrease the calculation error. Moreover, checking the IC would be a good practice to confirm that sonication purged the inorganic carbon.

Recalibration and maintenance have been performed on the device after the problem has been detected as well as all the samples had been used, therefore it was not possible to experimentally confirm that the 2nd dataset gives the correct values. It would be necessary to carry out these analyzes in duplicate in the future to eliminate the measurement error. Moreover, a new study suggests the sonication may decrease the purgeable organic carbon which contributes to the TC values [65]. Investigation of the effect of sonication on the biomass carbon concentration should be considered. If the change in organic carbon would be observed, ultrasound treatment should be avoided. Instead, an inorganic carbon (IC) measurement in TOC analyser should be introduced.

To further acknowledge the incorrectness of data, the carbon molecular content was compared with literature. The biomass molecular formula of autotrophically grown *P. denitrificans* is  $\text{CH}_{2.05}\text{O}_{0.77}\text{N}_{0.23}$ , according to [reference], giving 40 % of carbon content per C-mol biomass [66]. In case of *C. necator* formula being  $\text{CH}_{1.74}\text{O}_{0.46}\text{N}_{0.19}$ , carbon accounts for 50 % of the 1 C-mol biomass [52]. The results presented in the Table 8 and Figure 14 give the carbon contents which are significantly different from the aforementioned values. Instead of 1 mol carbon per 1 mol biomass the obtained numbers are completely different.

### 5.3. Nitrogen content of the cell

In terms of the TN data, the peaks follow predicted measurement behaviour with the first underestimated value, which is corrected with the calibration curve in the following peaks (Figure 26). Additionally, the TN method is highly accurate when considering 2-3 % deviations in standard values measurement (Appendix 1).

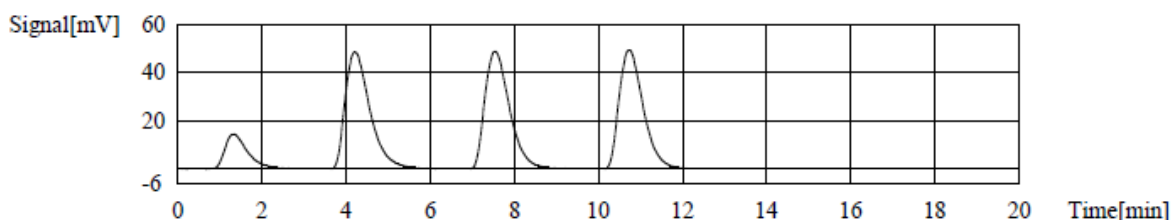


Figure 26 Example of obtained TN peak of culture supernatant sample.

Although, the negative change of nitrogen concentration in some samples including *H. flava* culture calls into question the consistency of the obtained results (Figure 15). Higher nitrogen content in the final supernatant sample resulting in the negative nitrogen content in the biomass could be explained by the release of extracellular protein, cell lysate or ammonium in the medium. In the study, ammonia was found to be reduced through sonication, thus decreasing total nitrogen. However, the  $\text{NH}_4^+$  ions cannot be vaporized, thus sample pre-treatment did not create the issue [67]. The exact cause of nitrogen increase remains unknown. Additionally, the initial total nitrogen measured in the supernatant does not correlate with the values obtained in  $\text{NO}_3^-$  and  $\text{NH}_4^+$  analyses. The TN data are 2- 3 times lower than nitrate-nitrogen and ammonia-nitrogen which were in the range of the concentrations calculated for the inoculated medium.

Measuring TN of broth should be done in addition to the supernatant as the data obtained in this work is not sufficient to accurately determine nitrogen content in the biomass. To avoid large deviation when accounting for dilution factor, applying as low sample dilution as it is possible is suggested.

Other remark on the data consistency concerns contamination of the supernatant samples with the presence of biomass. Supernatant was obtained by centrifuging sample, though filtering through  $0.2 \mu\text{m}$  filter might provide higher purity of the sample.



The proposed alternative carbon measurement methods include CHN analysers simultaneously identifying hydrogen, nitrogen, and carbon content of the cell. X-ray microanalysis (XRMA) coupled with a transmission electron microscope (TEM) has also been mentioned as a way to find carbon, nitrogen and phosphorus ratios in the cell [68]. If these techniques are available, it would be beneficial to run the analyses and compare their accuracy with TOC analyser. In terms of total nitrogen determination alternatives, the Automatic Kjeldahl Apparatus utilizing Kjeldahl digestion has been applied to quantify nitrogen and proteins in the cell [69].

#### **5.4. Protein content**

As shown in the Table 9, the protein content of individual strains has a wide spread of the values. All the results of *H. flava* are above 100 %, therefore none of them provide even an approximate realistic value. Looking at *P. denitrificans* samples, O1 has given  $82.2 \pm 2.6$  %, which compared to 67-73 % protein content determined in the autotrophic cultivation study is deviated by around 15 % [66]. In the autotrophic study on *C. necator*, the protein content was estimated to reach  $75 \pm 0.6$  % [24]. The results from serum bottle cultivation were all above 100 %, however protein determined from the batch culture had  $58.4 \pm 3.5$  % which is closer to the mentioned value. Unfortunately, there was no data available on *S. barnesii* and *H. flava* protein content.

The previous test attempts on *C. necator* which were not included in the final results also provided protein concentrations in the range of 0.2-0.4 g/L (Appendix 1). The Lowry protein assay appears to give consistent concentrations of the cell lysate solutions. Furthermore, the method seems suitable for low protein concentrations as the calibration curve with a high correlation coefficient was used. The samples pre-treatment included washing out the supernatant after centrifugation and resuspending the pellets to exclude the interference of salts. Chosen lysing matrix and applied rotation was sufficient to obtain the cell lysate. To conclude, the result reliability issue is caused by the incorrect BM concentration measurements, which distorted protein content from the expected range.

#### **5.5. Gaseous substrates consumption**

The gas mixture was supplied to the experimental bottles using MFC over the control of MS. It has to be mentioned that the initial gas contents measured with GC did not completely coincide with the values recorded in MS. Due to the fact that MS does not measure the gas samples continuously and MFC supply the gas with small flow variation ( $\pm 2$  ml/min), the gas contents varied slightly between samples, causing the variance in the initial GC results.

Furthermore, the manometer measurement error was around 2 kPa, which compared to the initial pressure in the bottles (101.325 kPa) gives not so significant deviation of 2 %. The initial GC was carried out before inoculation, thus the gas headspace at that time was 103 ml. However, injecting the inoculum and further sampling could have changed the liquid volume. The only available way to inoculate was to use syringes to add 4 ml and thereafter draw a 4 ml sample for analyses. The syringes did not have very accurate volume markings; thus, the volumetric error of sampling could be more significant than expected. The change in volume affected the pressure in the headspace. It is also worth mentioning that temperature of samples could also affect the pressure, as the samples were transferred to a different building for the analysis, hence they were sampled at temperature lower by about 10 °C. Moreover, possibility of the gas leakage during cultivation cannot be completely excluded, considering the low change in gas concentration in negative controls. All these factors have contributed to the measurement error and affected the gas consumption result.

Due to the fact that oxygen and hydrogen peaks were overlapping, peaks were not automatically assigned in the Chromeleon software processing GC data. Manual annotation is subjected to greater error than the automatic processing, what could affect the difference in concentration between initial and final samples. The higher the concentration of hydrogen is applied, the greater the area will overlap with oxygen peak. At the expense of increasing gas-liquid mass transfer of hydrogen the accuracy of peak annotation will decrease.

According to Figure 17, the oxygen consumption has occurred in all the aerobic samples at higher level for *C. necator*, *H. flava*, *P. denitrificans* and significantly lower in *S. barnesii* cultures. Hydrogen

consumption has also been observed at different levels, while an anomaly happened in *S. barnesii* samples which show no hydrogen consumption (Figure 18). It is contradictory to the growth increment of this strain. There were no other possible electron donors in the medium, which casts doubt on the reliability of this measurement. The average molar increase of hydrogen in those samples was between 0.5-1 mol (Appendix 1). The reasonable explanation for those results could be an incorrectly annotated hydrogen peak which overlapped with the oxygen, increasing the inaccuracy of data evaluation. The next issue was the decrease of nitrogen concentration in the gas headspace up to 30 % (Figure 17). With the consumption of other gases accompanied by the denitrification process, nitrogen concentration should have increased. Unfortunately, the change of nitrogen amount could not be explained due to insufficient evidence.

CO<sub>2</sub> was not measured as it would involve using the separate GC method. It would be advantageous to control its consumption to get better insight into changes occurring in the gas mixture. Therefore, the additional protocol would be recommended to obtain these data and further compare them with carbon content in the biomass to see if the rates of biomass correspond to CO<sub>2</sub> consumption.

To conclude, improvement of accuracy can be done by better volume control over the liquid inserted and drawn from the bottles. Moreover, adjusting the gas concentrations to completely separate the GC peaks. Finally, introducing a control gas which cannot be produced or consumed by bacteria such as helium and measuring CO<sub>2</sub> concentration would allow accurate determination of gas composition.

## 5.6. Ammonia yield

From the Figure 20, it can be observed that correlation between ammonium consumption and increment of biomass was not found in all the samples. NH<sub>4</sub><sup>+</sup> was assimilated into the biomass in certain aerobic samples of *H. flava*, *C. necator* and *S. barnesii*. From the anaerobic samples of *S. barnesii*, low production yield instead of the consumption was expected, as the result of DNRA. However, the consumption occurred in the anaerobic cultures, indicating denitrification process. The data did not correspond to the total nitrogen results. However, the initial ammonium-nitrogen concentrations were more in line with the calculated nitrogen content in the medium than the TN values.

Most concerning data related to the ammonium production yield in the aerobic samples, as shown in the Figure 21. Ammonium production should not occur in the aerobically growing *C. necator* and *P. denitrificans* samples, due to the lack of nitrate reduction process. Besides the DNRA, ammonium increase in the medium could be associated with death of bacteria, which is not the case accounting for the biomass concentrations data. Diazotrophy is not characteristic for HOB, therefore the measurement error must have occurred. Applying the suitable dilution factor in the colorimetric assay is the key to obtain reliable data. Even though the initial and final samples had the same dilution factor, the mere fact that they were diluted 16 times may have multiplied the error in the concentration calculation.

It has to be mentioned that the dilution factor of 4 for the anaerobic samples was initially chosen due to the expected residual amounts of ammonium in medium which would not exceed 10 % of the NH<sub>4</sub><sup>+</sup> in the aerobic samples. It resulted in bright yellow colour that indicates the lack of ammonium in the sample. Not applying the dilution in the final anaerobic sample allowed to develop the light green colour characteristic for the reaction with NH<sub>4</sub><sup>+</sup>. It was assumed that for the anaerobic cultures no dilution is needed as it also helps avoiding the error increasing when multiplying the OD by the dilution factor.

Regarding the unexpected ammonium yield values, adding only half of the 20 mM NH<sub>4</sub>Cl used in the experiment and adjusting the dilution to the lowest possible could decrease the measurement error. Additionally, performing the ammonium analysis in the AQ nutrient analyser would be a good option, resulting in more data for comparison.

## 5.7. Nitrate yield

Contrary to the expected behaviour of the anaerobic cultures, nitrate consumption has not been observed in every anaerobic sample. Given yields of NO<sub>3</sub> on the biomass differ significantly between

biological replicates of the same strain, including 6-fold difference between *H. flava* yields and 13-fold difference within *S. barnesii* samples, as seen in the Figure 19.

The yields are considerably affected by the deviations calculated for the initial and final concentrations. The difference between the duplicates of each initial sample ranged between 100-500 mg/L, accounting for less than 5 % of deviation. On the other hand, the difference in the final sample duplicates were spanned between 100-2000 mg/L, reaching up to 15 % of the standard deviation (Appendix 1). The larger deviation in the final samples is the main cause of data unreliability, which accounts for the high standard error of the yield reaching around 66-67 % of a total value (Figure 19).

Regarding the magnitude of  $\text{NO}_3^-$  consumption against its initial concentration in the samples, less than 30 % of that initial amount was consumed (Appendix 1). The low difference may have been more prone to the measurement error.

Considering the order of magnitude of the concentrations difference and the high standard deviation values, it can be concluded that the results are inconsistent and cannot be deemed accurate.

It has to be noted that consumption of  $\text{NO}_3^-$  occurred in the anaerobic *C. necator* samples even though the yield is expressed as 0, as there was no biomass growth. The biological explanation to nitrate production in the sample was not found. Therefore, the measurements were burdened with high deviation what resulted in the invalid data.

Initially the colorimetric method was planned to be applied, however due to inability of obtaining accurate calibration curve the method was changed to presumably more accurate AQ2 analyser which is more automated. However, this method proved to be subjected to a large measurement variation. The range of analyser is up to 15 mg of N- $\text{NO}_3$ , thus all the samples had to be diluted 180 times, what contributed to the error range. An experiment with a lower initial  $\text{NO}_3^-$  concentration would help decreasing the measurement error. Decreasing the nitrate concentration in medium to 5-10 mM would be a feasible option [26]

## 5.8. Growth rate in the batch cultivation

The *C. necator* culture growth over 72 hours appeared to be linear. No transition from the lag to exponential growth and the stationary phase was observed, according to the Figure 22. The linear growth curve indicates that the gas-liquid mass transfer was not efficient. Hydrogen was poorly transferred from the gas bag to the reactor headspace, what could be seen on the hydrogen saturation plot presented in the Figure 27. Therefore, bacterial growth was substrate limited. However, not enough samples were taken to ultimately determine the growth pattern, as the culture did not reach the stationary phase when harvested. Greater culture broth volume to take more samples and longer cultivation time could provide better insight into autotrophic growth rate. Nonetheless, the reactor setup might not provide the suitable conditions for exponential growth, thus the adjustments are needed. Gas mixture transfer from the external bag to the reactor headspace has to be improved.

In the study on aerobic chemolithotrophic growth of *C. necator*, obtained growth rates ranged from 0.011 to 0.094 (1/h). The average growth rate of a batch culture in this experiment reached 0.021 (1/h), which classifies it within the lower limit of the growth rates [70].

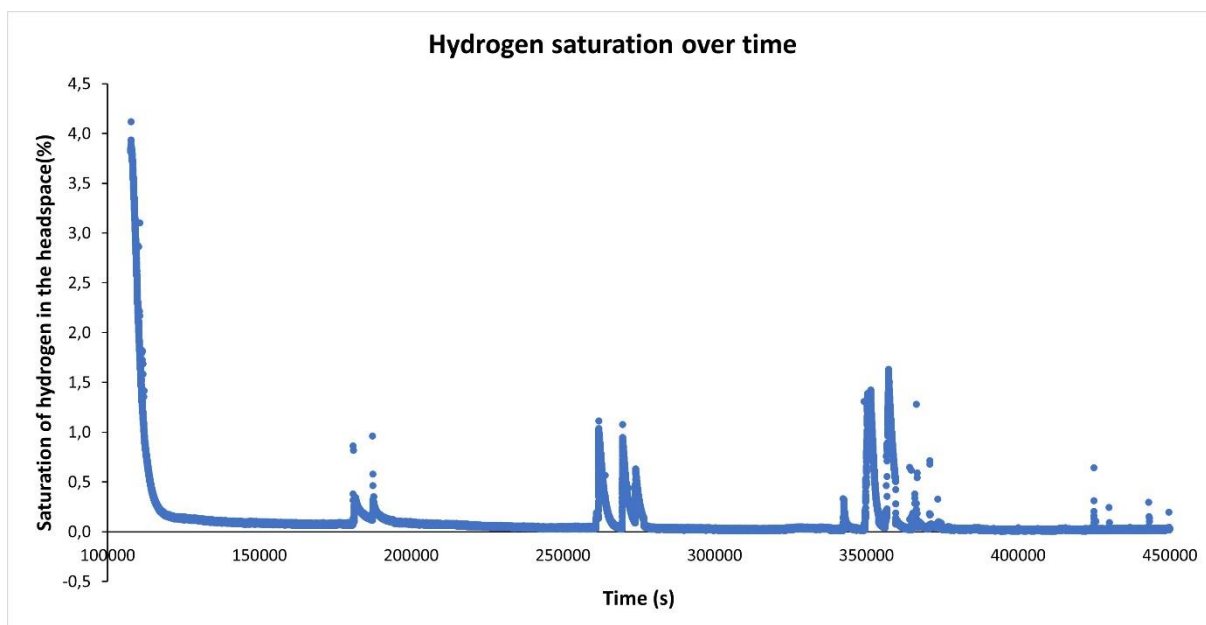


Figure 27 Hydrogen saturation in the reactor headspace over time.

### 5.9. Biomass formation stoichiometry and energy cost

Due to the inconsistency of substrate consumption rates and biomass concentrations, the obtained biomass formation equation made no biological sense. Balancing the equation with water and protons has resulted in their negative rates. Moreover, in several samples the rates of substrates indicated production as well as the compounds were consumed in the samples with no biomass growth. The same situation applies to the enthalpy of the reaction, directly related to stoichiometric coefficients. The realistic values could not be established.

## 6. Conclusion

---

The thesis aimed to choose the most productive HOB cultivation method considering the energetically efficient respiration pathway and the best performing bacteria strain. The selection concerned 4 facultatively aerobic HOB species, which were subjected to hydrogenotrophic growth in the aerobic and anaerobic conditions. The comparison covered the yields of hydrogen on the biomass and the energy cost associated with the biomass production. To determine their values, the experimental setup was designed to cultivate the bacteria and further analyse the consumption of the electron donor and acceptor as well as the nitrogen and carbon source. Successful data integration into the final results depended on the qualitative assessment of the methods.

The experimental design consisted of the HOB cultivation in closed serum bottles followed by the measurements of gaseous substrates consumption, total carbon and total nitrogen content in the cell, ammonium and nitrate concentration. The species examined were *H. flava*, *P. denitrificans*, *S. barnesii* and *C. necator*, respectively. The culture broth was used to determine the biomass concentration and protein content. Moreover, the batch reactor cultivation was performed on *C. necator* strain to check how the batch gas phase operation mode can be implemented as well as the growth rate of the HOB culture in upscaled cultivation system. The results and methods which were used for the analyses were subsequently evaluated.

It has been generally observed that the results of the analyses provided the inconsistent results, even though the data should have been interconnected and complement each other. The TC content did not align with the biomass concentration, giving the carbon amount considerably higher than the calculated cell dry weight. Furthermore, the TN concentration in the initial and final samples did not correspond to the measured ammonium and nitrate nitrogen values. Consumption of the substrates was observed in the samples where no biomass increment was noted. Moreover, the consumption of compounds such as  $N_2$  was measured, despite the lack of a chemical or biological conversion behind it. On the other hand, there was an unexpected increase of substrate concentrations in several samples instead of consumption considering the nitrogen containing compounds, hydrogen and oxygen gas. Similarly, the measurements of one parameter with two methods, as in the case of biomass concentration, gave contradictory results. The discrepancy of the data is supported by a large standard deviation or measured standard error. Therefore, all the obtained results were subjected to significant inconsistency and lack of reliability. The measurement errors prevented achieving the main goal of the thesis, as the yields and enthalpies could not be established. The energy efficiency was not assessed as well.

However, the first two research questions were answered. The experimental setup occurred to be unsuitable in the current form. The experimental setup was lacking some analyses which could improve the data accuracy as well as the protocols were burdened with several issues both during cultivation and sample analysis. The outcome data was found to be inconsistent and unreliable, thus it cannot be validated. To conclude, the design setup needs improvements to achieve the thesis aim.

Referring to the improvement suggested in the discussion part, it would be beneficial to upscale the volume of serum bottles to have more culture broth for sampling. Increasing the number of replicates will improve the accuracy. It is important to correctly determine the biomass concentration. Cell dry weight should be determined both in the initial and final samples along with the OD control with the growth control samples. The cultivation period should be prolonged to at least 3 weeks to observe larger change in concentration and substrate consumption in the anaerobic samples. Furthermore, collaboration with the microbiology department will facilitate preparation of the cultivation setup. What is more, applying lower  $NO_3^-$  and  $NH_4^+$  concentrations along with the dilution factor adjustments may decrease the measurement error. To improve the accuracy of GC readings, applying the hydrogen concentration between 10-15 % while keeping the oxygen concentration in the gas mixture below 6 % should separate the peak reading, facilitating the peak annotation. To ensure consistency of GC data calculation, the liquid sampling volumes need to be more controlled. Finally,  $CO_2$  assay is recommended to be implemented in the GC measurements.

# Acknowledgements

---

Special thanks to Carlos Serrano Fajardo for inspiring supervision over the thesis work. The meetings and insightful discussions shaped the final experimental design. I would also like to express my gratitude to Giuseppe and Ruud Weusthuis for their support throughout the project as well the proposed ideas and constructive critique which turned out to be very useful. I would like to thank Sebastiaan Haemers for technical support and providing quick solutions to emerging laboratory issues.

## References

---

1. Duku, C., Alho, C., Leemans, R., Groot A. , *Climate change and food system activities: a review of emission trends, climate impacts and the effects of dietary change*, in *IFAD Research Series 72*, R. IFAD, Editor. 2022.
2. Leaver, J.D., *Global food supply: a challenge for sustainable agriculture*. *Nutrition Bulletin*, 2011. **36**(4): p. 416-421.
3. Henchion, M., et al., *Future Protein Supply and Demand: Strategies and Factors Influencing a Sustainable Equilibrium*. *Foods*, 2017. **6**(7): p. 53.
4. FAO, *World Food and Agriculture – Statistical Yearbook 2022*, in *FAO Statistical Yearbook – World Food and Agriculture*. 2022: Rome, Italy. p. 382.
5. Poore, J. and T. Nemecek, *Reducing food's environmental impacts through producers and consumers*. *Science*, 2018. **360**(6392): p. 987-992.
6. Sharif, M., et al., *Single cell protein: Sources, mechanism of production, nutritional value and its uses in aquaculture nutrition*. *Aquaculture*, 2021. **531**.
7. Ritala, A., et al., *Single Cell Protein-State-of-the-Art, Industrial Landscape and Patents 2001-2016*. *Front Microbiol*, 2017. **8**: p. 2009.
8. Pander, B., et al., *Hydrogen oxidising bacteria for production of single-cell protein and other food and feed ingredients*. *Engineering Biology*, 2020. **4**(2): p. 21-24.
9. Leger, D., et al., *Photovoltaic-driven microbial protein production can use land and sunlight more efficiently than conventional crops*. *Proc Natl Acad Sci U S A*, 2021. **118**(26).
10. Linder, T., *Making the case for edible microorganisms as an integral part of a more sustainable and resilient food production system*. *Food Security*, 2019. **11**(2): p. 265-278.
11. Pikaar, I., et al., *Carbon emission avoidance and capture by producing in-reactor microbial biomass based food, feed and slow release fertilizer: Potentials and limitations*. *Science of The Total Environment*, 2018. **644**: p. 1525-1530.
12. Sillman, J., et al., *Bacterial protein for food and feed generated via renewable energy and direct air capture of CO<sub>2</sub>: Can it reduce land and water use?* *Global Food Security*, 2019. **22**: p. 25-32.
13. Aragno, M. and H.G. Schlegel, *The Hydrogen-Oxidizing Bacteria*. 1981, Springer Berlin Heidelberg. p. 865-893.
14. Keith, D.W., et al., *A Process for Capturing CO<sub>2</sub> from the Atmosphere*. *Joule*, 2018. **2**(8): p. 1573-1594.
15. Ghavam, S., et al., *Sustainable Ammonia Production Processes*. *Frontiers in Energy Research*, 2021. **9**.
16. Garcia Martinez, J.B., et al., *Potential of microbial protein from hydrogen for preventing mass starvation in catastrophic scenarios*. *Sustain Prod Consum*, 2021. **25**: p. 234-247.
17. Oorde, R.v., *Food from air: an investigation into energy efficiency of single-cell protein production using different microbial electron acceptors*, in *Department of Bioprocess Engineering*. 2022, Wageningen University.
18. Yu, J. and Y. Lu, *Carbon dioxide fixation by a hydrogen-oxidizing bacterium: Biomass yield, reversal respiratory quotient, stoichiometric equations and bioenergetics*. *Biochemical Engineering Journal*, 2019. **152**.
19. Miyahara, Y., et al., *Continuous Supply of Non-Combustible Gas Mixture for Safe Autotrophic Culture to Produce Polyhydroxyalkanoate by Hydrogen-Oxidizing Bacteria*. *Bioengineering*, 2022. **9**(10): p. 586.
20. Hu, X., P. Vandamme, and N. Boon, *Co-cultivation enhanced microbial protein production based on autotrophic nitrogen-fixing hydrogen-oxidizing bacteria*. *Chemical Engineering Journal*, 2022. **429**: p. 132535.
21. Tanaka, K., et al., *Production of poly(D-3-hydroxybutyrate) from CO<sub>2</sub>, H<sub>2</sub>, and O<sub>2</sub> by high cell density autotrophic cultivation of *Alcaligenes eutrophus**. *Biotechnology and Bioengineering*, 1995. **45**(3): p. 268-275.

22. ToolBox, E. *Solubility of Gases in Water vs. Temperature*. 2008 [cited 2023 6.02]; Available from: [https://www.engineeringtoolbox.com/gases-solubility-water-d\\_1148.html](https://www.engineeringtoolbox.com/gases-solubility-water-d_1148.html).
23. Rambhujun, N., et al., *Renewable hydrogen for the chemical industry*. MRS Energy & Sustainability, 2020. **7**(1).
24. Vrauwdeunt, G.A., *Food from thin air; an outlook on microbial protein production by hydrogen oxidizing bacteria using modeling and laboratory experiments*, in *Department of Bioprocess Engineering*. 2022, Wageningen University: Wageningen University. p. 69.
25. Claassens, N.J., et al., *Making quantitative sense of electromicrobial production*. Nature Catalysis, 2019. **2**(5): p. 437-447.
26. Strohm, T.O., et al., *Growth yields in bacterial denitrification and nitrate ammonification*. Appl Environ Microbiol, 2007. **73**(5): p. 1420-4.
27. Kraft, B., M. Strous, and H.E. Tegetmeyer, *Microbial nitrate respiration--genes, enzymes and environmental distribution*. J Biotechnol, 2011. **155**(1): p. 104-17.
28. Bueno, E., et al., *Bacterial Adaptation of Respiration from Oxic to Microoxic and Anoxic Conditions: Redox Control*. Antioxidants & Redox Signaling, 2012. **16**(8): p. 819-852.
29. Simon, J. and M.G. Klotz, *Diversity and evolution of bioenergetic systems involved in microbial nitrogen compound transformations*. Biochimica et Biophysica Acta (BBA) - Bioenergetics, 2013. **1827**(2): p. 114-135.
30. Chegg. *Redox Tower*. [cited 2023; Available from: <https://www.chegg.com/homework-help/questions-and-answers/12-according-redox-tower-picture-following-best-electron-donor-co2-mno2-ch4-nh4-correct-an-q15861995>].
31. Chen, J. and M. Strous, *Denitrification and aerobic respiration, hybrid electron transport chains and co-evolution*. Biochim Biophys Acta, 2013. **1827**(2): p. 136-44.
32. Calisto, F., et al., *Mechanisms of Energy Transduction by Charge Translocating Membrane Proteins*. Chemical Reviews, 2021. **121**(3): p. 1804-1844.
33. WILHELM, O., *Improvements in the Manufacture of Nitric Acid and Nitrogen Oxides*. 1902: Germany.
34. Fay, P., *Oxygen relations of nitrogen fixation in cyanobacteria*. Microbiol Rev, 1992. **56**(2): p. 340-73.
35. Oshiki, M., et al., *Growth of nitrite-oxidizing *Nitrospira* and ammonia-oxidizing *Nitrosomonas* in marine recirculating trickling biofilter reactors*. Environmental Microbiology, 2022. **24**(8): p. 3735-3750.
36. Kohlmann, Y., et al., *Coping with Anoxia: A Comprehensive Proteomic and Transcriptomic Survey of Denitrification*. Journal of Proteome Research, 2014. **13**(10): p. 4325-4338.
37. Cramm, R., *Genomic View of Energy Metabolism in *Ralstonia eutropha* H16*. Microbial Physiology, 2009. **16**(1-2): p. 38-52.
38. Jiang, Y., et al., *Synchronous microbial vanadium (V) reduction and denitrification in groundwater using hydrogen as the sole electron donor*. Water Research, 2018. **141**: p. 289-296.
39. Liu, X., et al., *Nitrate removal from low carbon-to-nitrogen ratio wastewater by combining iron-based chemical reduction and autotrophic denitrification*. Bioresour Technol, 2020. **301**: p. 122731.
40. Willems, A., et al., *Hydrogenophaga, a New Genus of Hydrogen-Oxidizing Bacteria That Includes *Hydrogenophaga flava* comb. nov. (Formerly *Pseudomonas flava*), *Hydrogenophaga palleronii* (Formerly *Pseudomonas palleronii*), *Hydrogenophaga pseudoflava* (Formerly *Pseudomonas pseudoflav**. International Journal of Systematic Bacteriology, 1989. **39**(3): p. 319-333.
41. Consortium, T.U., *UniProt: the Universal Protein Knowledgebase in 2023*. 2023.
42. Harms, N. and R.J.M. Van Spanning, *C1 metabolism in *Paracoccus denitrificans*: Genetics of *Paracoccus denitrificans**. Journal of Bioenergetics and Biomembranes, 1991. **23**(2): p. 187-210.
43. Ye, J., et al., *Performance and mechanism of carbon dioxide fixation by a newly isolated chemoautotrophic strain *Paracoccus denitrificans* PJ-1*. Chemosphere, 2020. **252**: p. 126473.



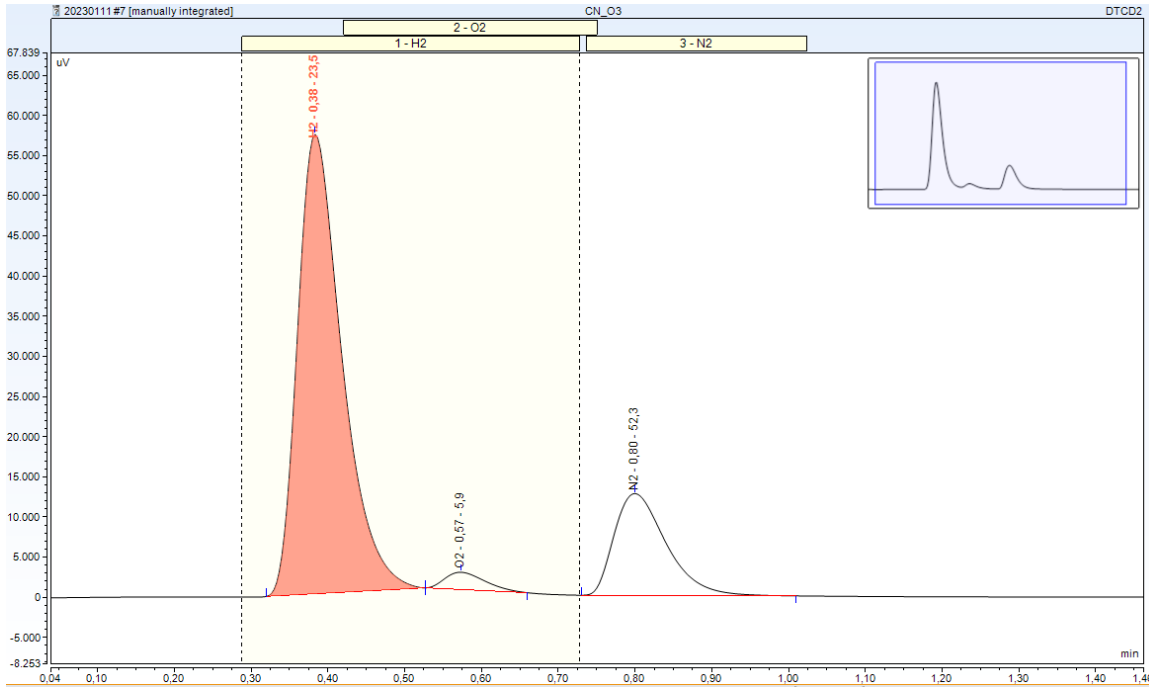
44. Gates, Andrew J., et al., *A composite biochemical system for bacterial nitrate and nitrite assimilation as exemplified by Paracoccus denitrificans*. *Biochemical Journal*, 2011. **435**(3): p. 743-753.
45. Bouchal, P., et al., *Unraveling an FNR based regulatory circuit in Paracoccus denitrificans using a proteomics-based approach*. *Biochim Biophys Acta*, 2010. **1804**(6): p. 1350-8.
46. Seyler Lauren, M., et al., *Carbon Assimilation Strategies in Ultrabasic Groundwater: Clues from the Integrated Study of a Serpentinization-Influenced Aquifer*. *mSystems*, 2020. **5**(2): p. e00607-19.
47. Knoche, W., *Chemical Reactions of CO<sub>2</sub> in Water*. 1980, Springer Berlin Heidelberg. p. 3-11.
48. Preiss, L., et al., *Alkaliphilic Bacteria with Impact on Industrial Applications, Concepts of Early Life Forms, and Bioenergetics of ATP Synthesis*. *Front Bioeng Biotechnol*, 2015. **3**: p. 75.
49. Bird, L.J., et al., *Serpentinimonas gen. nov., Serpentinimonas raichei sp. nov., Serpentinimonas barnesii sp. nov. and Serpentinimonas maccroryi sp. nov., hyperalkaliphilic and facultative autotrophic bacteria isolated from terrestrial serpentinizing springs*. *International Journal of Systematic and Evolutionary Microbiology*, 2021. **71**(8).
50. Li, H., et al., *Integrated Electromicrobial Conversion of CO<sub>2</sub> to Higher Alcohols*. *Science*, 2012. **335**(6076): p. 1596-1596.
51. Lambauer, V. and R. Kratzer, *Lab-Scale Cultivation of Cupriavidus necator on Explosive Gas Mixtures: Carbon Dioxide Fixation into Polyhydroxybutyrate*. *Bioengineering*, 2022. **9**(5): p. 204.
52. Tiemeyer, A., H. Link, and D. Weuster-Botz, *Kinetic studies on autohydrogenotrophic growth of Ralstonia eutropha with nitrate as terminal electron acceptor*. *Applied Microbiology and Biotechnology*, 2007. **76**(1): p. 75-81.
53. Reilly, S., *THE CARBON DIOXIDE REQUIREMENTS OF ANAEROBIC BACTERIA*. *Journal of Medical Microbiology*, 1980. **13**(4): p. 573-579.
54. Garcia-Gonzalez, L., et al., *Sustainable autotrophic production of polyhydroxybutyrate (PHB) from CO<sub>2</sub> using a two-stage cultivation system*. *Catalysis Today*, 2015. **257**: p. 237-245.
55. Windhorst, C. and J. Gescher, *Efficient biochemical production of acetoin from carbon dioxide using Cupriavidus necator H16*. *Biotechnology for Biofuels*, 2019. **12**(1).
56. Waterborg, J.H., *The Lowry Method for Protein Quantitation*. 2009, Humana Press. p. 7-10.
57. ThermoFisher, *Protein assay technical handbook. Tools and reagents for improved quantitation of total or specific proteins*. 2017. p. 60.
58. Wang, Q.-H., et al., *Methods for the detection and determination of nitrite and nitrate: A review*. *Talanta*, 2017. **165**: p. 709-720.
59. U.S.EPA, *Method 350.1: Nitrogen, Ammonia (Colorimetric, Automated Phenate)*, R. 2.0, Editor. 1993: Cincinnati, OH.
60. Zoulias, E., et al., *A Review on Water Electrolysis*. *TCJST*, 2004. **4**: p. 41-71.
61. Appl, M., *Ammonia*. *Ullmann's Encyclopedia of Industrial Chemistry*, 2006.
62. Heldal, M., S. Norland, and O. Tুমyr, *X-ray microanalytic method for measurement of dry matter and elemental content of individual bacteria*. *Appl Environ Microbiol*, 1985. **50**(5): p. 1251-7.
63. Koike, I. and A. Hattori, *Growth Yield of a Denitrifying Bacterium, Pseudomonas denitrificans, under Aerobic and Denitrifying Conditions*. *Journal of General Microbiology*, 1975. **88**(1): p. 1-10.
64. Wang, Y., et al., *Quantification of the Filterability of Freshwater Bacteria through 0.45, 0.22, and 0.1 μm Pore Size Filters and Shape-Dependent Enrichment of Filterable Bacterial Communities*. *Environmental Science & Technology*, 2007. **41**(20): p. 7080-7086.
65. Kim, J.-W., et al., *Identification of the cause of the difference among TOC quantitative methods according to the water sample characteristics*. *Science of The Total Environment*, 2023: p. 162530.
66. Dou, J., et al., *Autotrophic, Heterotrophic, and Mixotrophic Nitrogen Assimilation for Single-Cell Protein Production by Two Hydrogen-Oxidizing Bacterial Strains*. *Applied Biochemistry and Biotechnology*, 2019. **187**(1): p. 338.

67. Ozturk, E. and N. Bal, *Evaluation of ammonia–nitrogen removal efficiency from aqueous solutions by ultrasonic irradiation in short sonication periods*. *Ultrasonics Sonochemistry*, 2015. **26**: p. 422-427.
68. Romanova, N.D. and A.F. Sazhin, *Relationships between the cell volume and the carbon content of bacteria*. *Oceanology*, 2010. **50**(4): p. 522-530.
69. Wang, H., et al., *Protein Nitrogen Determination by Kjeldahl Digestion and Ion Chromatography*. *Journal of Pharmaceutical Sciences*, 2016. **105**(6): p. 1851-1857.
70. Yu, J. and P. Munasinghe, *Gas Fermentation Enhancement for Chemolithotrophic Growth of *Cupriavidus necator* on Carbon Dioxide*. *Fermentation*, 2018. **4**(3).

# Appendices

The data obtained in this research can be accessed in the supplementary data file:

Appendix 3 [HOB cultivation and measurements .xlsx](#)



Appendix 2 An example of manually annotated peaks in Chromeleon software.

## AQ2 Tray Report

Software Version: 2.1.4  
 Report Requested By: seal  
 Date & Time: 2023-01-20 13:17:57  
 Tray Number: 12  
 Tray Name: 23.01.19 NG 2nd3rd run

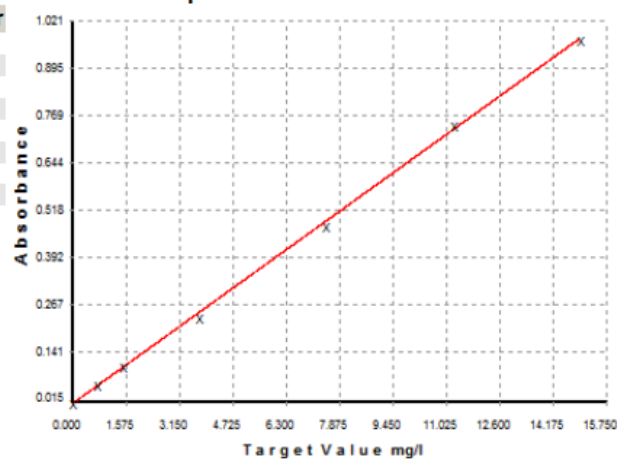
### NO3\_15

#### Calibration Chart

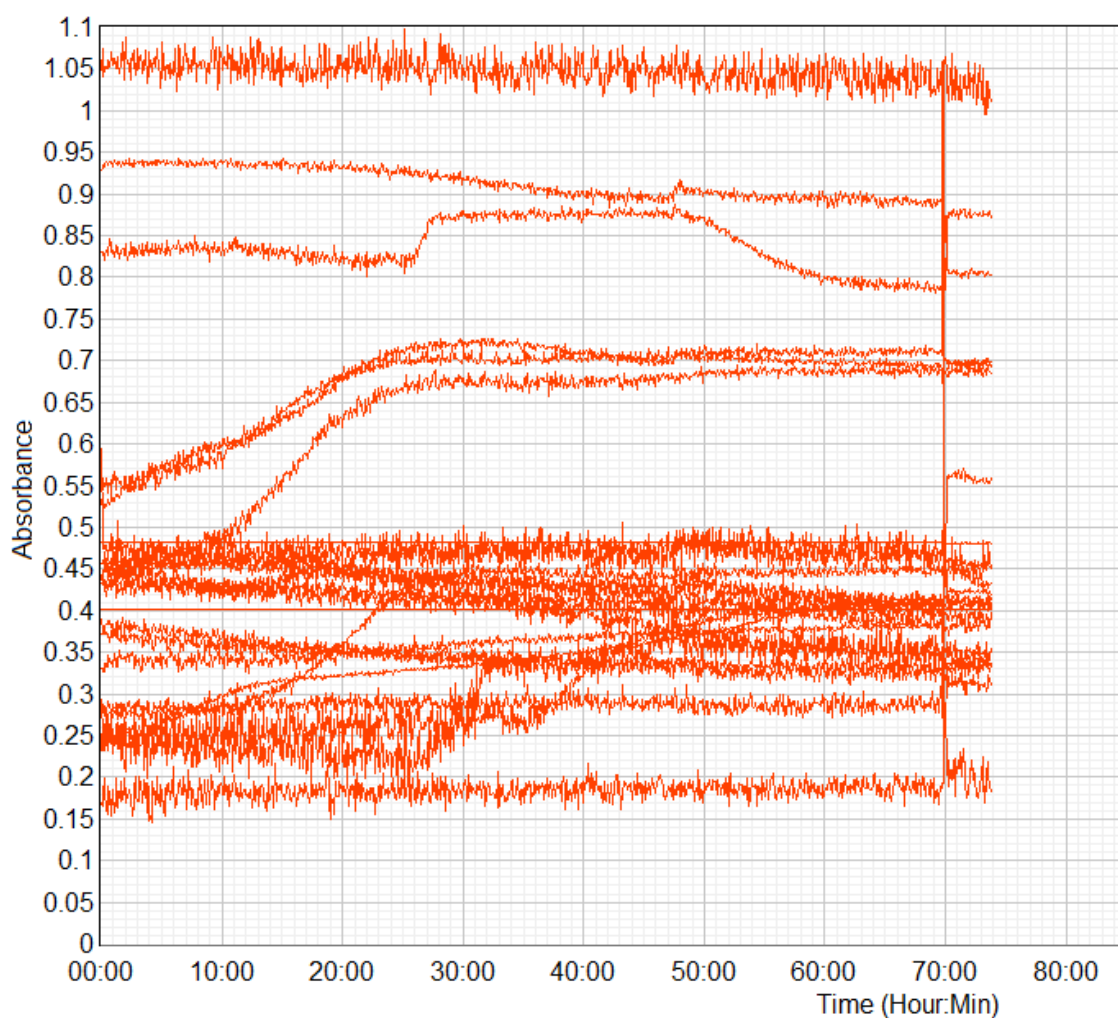
Type	Absorbance	Calc mg/l	Target mg/l	% Error
S1	0.0155	0.0736	0.0000	
S90	0.0635	0.8206	0.7500	9.42
S91	0.1089	1.5277	1.5000	1.85
S92	0.2400	3.5677	3.7500	-4.86
S93	0.4821	7.3368	7.5000	-2.18
S94	0.7471	11.4607	11.2500	1.87
S95	0.9721	14.9629	15.0000	-0.25
S0	0.0178	0.1091	0.0000	

Polynomial Order: 1  
 Correlation Coefficient: 0.9997  
 Carryover(%): 0.2  
 Calibration equation:  $y = bx + a$   
 y = Concentration mg/l  
 x = Measured absorbance  
 a = -1.675228E-001  
 b = 1.556445E+001  
 Date & Time: 2023-01-19 12:33:54

#### Calibration Graph



Appendix 1 Nitrate assay automatic standard calibration results.



Appendix 4 Overview of the OD740 continuous measurement of *H. flava*, *P. denitrificans* and *S. barnesii* cultures.

Reactor Type	1 litre, dished bottom
Inner Diameter	95 mm
Inner Height (maximum)	200 mm
Liquid height (working volume)	150 mm
Overall height reactor	290 mm
Total Volume	1.25 litre
Working Volume	0.9 litre
Minimal Working volume	0.3 litre

Appendix 5 Dimensions of the CSTR used in the batch experiment [24]

